Nonlinear Wave Theory for Dynamics of Binary Distillation Columns

Yng-Long Hwang
Union Carbide Chemicals and Plastics Company Inc., South Charleston, WV 25303

A major difficulty in control of distillation columns stems from their nonlinear behavior, especially of columns producing high-purity products. Based on a previous development that adapted fixed-bed theories to simple countercurrent processes, this study has established a nonlinear wave theory for the nonlinear and distributed dynamics of binary distillation columns by including the effects of reflux, reboil, and combination of sections. This theory clearly elucidates the intriguing dynamic behavior of distillation columns such as high steady-state gains, large response lags, strong dependence of dynamics on the magnitudes and directions of disturbances, and asymmetric dynamics of the transitions between two steady states. It also underlines the inadequacy of conventional linearized models for high-purity columns. With fairly simple mathematics, this nonlinear wave approach may be useful for model development, control system design, dual-composition control, and feedforward control.

Introduction

Distillation is the most widely practiced separation process in the chemical and petroleum industries. Recently, the increasing demands of high product quality, minimal waste generation, and low energy consumption have called for better performance and tighter control of distillation columns. As Gould (1969) emphasized 20 years ago, the process itself is the main focus of chemical process control. In the past few decades, however, chemical control engineers have paid more attention to column control systems than to distillation columns themselves. Although the nonlinear and distributed character ("distributed" in this article is interpreted from the point of view of an entire process) of distillation columns has long been recognized, distillation dynamics has been modeled with linearized and lumped approaches in conventional control system design to fit into the linear control theory. Control systems implemented using such an approach have functioned acceptably for columns with products of low to moderate purity, but have encountered difficulties recently when applied to high-purity columns, especially for control of compositions of both overhead and bottom products (dual-composition control).

Distillation columns producing high-purity products have become more and more important owing to the growing demands of such products and the requirement of waste reduction. By nature, a high-purity column exhibits a highly nonlinear, distributed character as reflected by its sharp composition and temperature profiles, because only a small portion of the column is utilized for the major separation while other parts are only responsible for refining the products. Such nonlinear dynamics has been realized for more than 30 years (Rose et al., 1956; Moczek et al., 1965; Mohr, 1965), and a few attempts were made to combat the associated control difficulties (Luyben, 1971, 1972; Gilles and Retzbach, 1980, 1983; Fuentes and Luyben, 1983; Kapoor et al., 1986; Kapoor and McAvoy, 1987; Skogestad and Morari, 1987, 1988; Marquardt, 1988; Alsop and Edgar, 1990). Although nonlinear dynamics has been successfully handled with linearization for many lumped processes, many problems have arisen in such an approach to distributed processes such as distillation columns. For lack of tight control, high purity of a distillate product has been achieved by over-refluxing at the cost of higher energy consumption (Douglas et al., 1979) and lower production rate; moreover, such a practice usually sacrifices the bottom product purity and, therefore is likely to incur additional expense for purification or disposal of the bottom product. To improve distillation control in general and dual composition control in particular, we need to have a better understanding of the nonlinear and distributed nature of distillation columns.

Nonlinear dynamic phenomena of distillation columns appearing in the computer simulations of earlier investigators include high steady-state gains, large response lags (time con-

stants in linear models), and strong dependence of gains and lags on the magnitudes and directions of disturbances (Luyben, 1971; Fuentes and Luyben, 1983; Kapoor et al., 1986; Skogestad and Morari, 1987). A more interesting phenomenon has been known as "asymmetric dynamics" (Rose et al., 1956; Moczek et al., 1965; De Lorenzo et al., 1972; Mizuno et al., 1972; Weigand et al., 1972; Stathaki et al., 1985), which refers to the difference in response times either for a steady state perturbed by a pair of step disturbances of the same magnitude but in opposite directions, or for the forward and reverse transitions between two steady states. The second type of dynamic asymmetry is more critical to distillation control. It was found that the transition departing from the steady state with maximum separation is always faster, and usually much faster, than the returning transition. This implies that the most desirable steady state is unfortunately the one most difficult to maintain. So far, few explanations have been given to these intriguing dynamic phenomena.

The objectives of this study are to obtain deeper insight into the nonlinear, distributed dynamics of distillation columns, and to establish a tool for model development, control system design, implementation of dual-composition control, and formulation of predictive (e.g., feedforward) control algorithms. For such purposes, this tool must well reflect the essential nonlinear and distributed nature of distillation columns within a concise mathematical framework. The approach employed views the movement of sharp profiles in distillation columns as nonlinear "waves" and adapts the nonlinear wave theory for fixed-bed sorption to distillation dynamics. The concept of wave propagation on distillation columns was discussed as early as 40 years ago, but early applications of the wave concept (Bowman and Briant, 1947; Jaswon and Smith, 1954; Lamb et al., 1961) ignored the nonlinear nature of distillation. Recently, Nandakumar and Andres (1981) applied the theory of multicomponent chromatography (Helfferich, 1968; Helfferich and Klein, 1970; Rhee et al., 1970) to a steady-state calculation of minimum reflux ratios for multicomponent distillation columns. Specifically on dynamics and control, several investigators intuitively exploited the phenomenon of movement of sharp temperature or composition profiles in high-purity columns, without utilizing the nonlinear wave theories advanced in other fields. Using the location of a sharp temperature profile as a controlled variable, Luyben (1972) pioneered a profile-position control strategy, which was later reinvented and applied to plant columns by Boyd (1975) and by Silberberger (1977), respectively. The work of Silberberger was fortified by Gilles and Retzbach (1980, 1983) with an improved moving-front model, and more recently by Marquardt (1985, 1988), who utilized the nonlinear wave concept to develop a novel model for binary distillation using the wave position and wave shape parameters as state variables. These studies, however, ignored the column-end effects, which are indeed critical to countercurrent processes as discussed in detail previously for gas absorbers (Hwang, 1987; Hwang and Helfferich, 1988). Instead of constructing a dynamic model or a control strategy, the present study is intended to provide a tool for these application purposes by elucidating the fundamental aspects of the nonlinear wave behavior in distillation columns. The theoretical development has proceeded on the basis of previous studies that adapted the wave theory for fixed-bed sorption to simple countercurrent processes (Hwang, 1987; Hwang and Helfferich, 1988) and clarified the physical course of the asymmetric dynamics in such operations (Hwang and Helfferich, 1989). The current work has extended the previous results to distillation columns by including the effects of reflux, reboil, and combination of sections. In this article, the discussion will be limited to binary distillation, to which the univariant (or single-solute) wave theory will be applied.

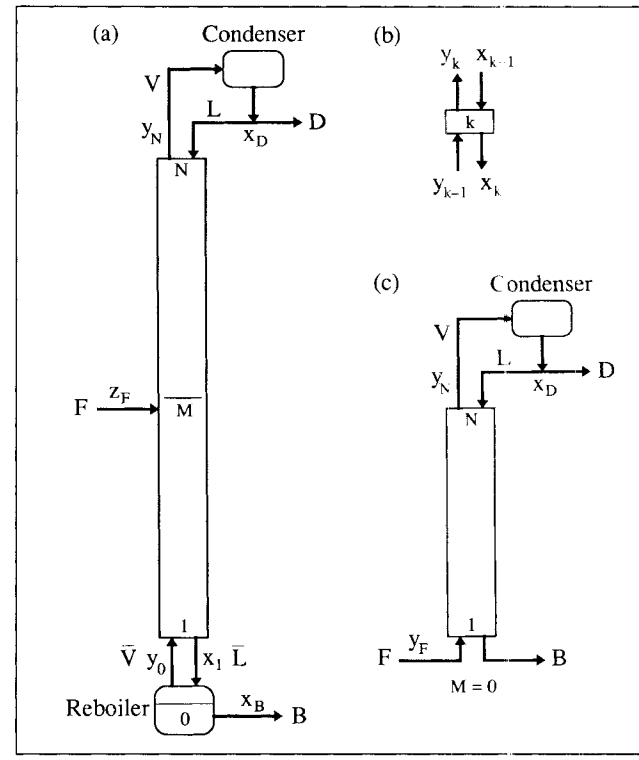

Figure 1. Example binary distillation columns.

a. Fractionating column; b. a typical plate; c. rectifying column

Some ideas on applying the nonlinear wave theory to distillation control are proposed, but detailed discussions of these applications are beyond the scope of the article. In addition to control applications, this theory may help design new columns or modify existing equipment so that distillation columns will be less sensitive to disturbances and thus easier to operate. The ability of supplementing conventional steady-state design techniques with dynamic information may bring us a step closer to the integration of equipment design and control system design.

Example System

Focusing on the fundamental behavior of distillation columns, the theoretical development will be exemplified by a simple prototype: binary distillation in a fractionating column of N plates with a single feed as shown in Figure 1a. The plates are counted upward with a typical plate k illustrated by Figure 1b; the reboiler is numbered as stage 0. A simple stagewise model has been established for the numerical simulation of the example column. This model assumes ideal equilibrium stages (plates and the reboiler), a total condenser, constant molar overflow, constant molar holdups of all plates with the

Table 1. Stagewise Model for Example Distillation Column

Material Balances	
Reboiler (stage 0)	$H_B\frac{dx_0}{dt}=\bar{L}x_1-\bar{V}y_0-Bx_0$
Stripping section ($k=1,2,\ldots,M-1$)	$H\frac{dx_k}{dt}+G\frac{dy_k}{dt}=\bar{L}(x_{k+1}-x_k)+\bar{V}(y_{k-1}-y_k)$
Feed plate (stage M)	$H\frac{dx_M}{dt}+G\frac{dy_M}{dt}=Lx_{M+1}-\bar{L}x_M+\bar{V}y_{M-1}-Vy_M+Fz_F$
Rectifying section ($k=M+1,\ldots,N$)	$H\frac{dx_k}{dt}+G\frac{dy_k}{dt}=L(x_{k+1}-x_k)+V(y_{k-1}-y_k)$
Total condenser (not a stage)	$H_D\frac{dx_D}{dt}=Vy_N-(L+D)x_D$
Equilibrium (a Formal Representation)	$y_k=f(x_k)$
Normalized Parameters and Variables	
Vapor-to-liquid holdup ratio	$r\equiv G/H$
Normalized reboiler holdup	$h_B\equiv H_B/NH$
Normalized condenser holdup	$h_D\equiv H_D/NH$
Normalized time	$\tau\equiv\frac{t}{NH/F}$
Normalized distance	$\sigma\equiv k/N$

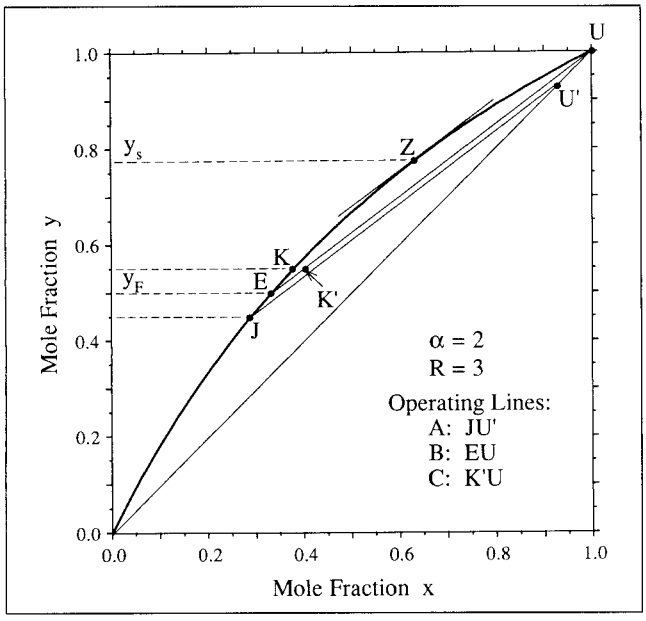

Figure 2. Equilibrium curve of binary system, operating lines of high-purity rectifying column, and composition points showing nonlinear wave concept.

same value, as well as constant liquid holdups and negligible vapor holdups of the reboiler and the condenser. Also, the energy balance equations are disregarded, and therefore the temperature is determined solely by the composition in each stage through the equilibrium relationship. These assumptions not only make the computation simple, but also direct our attention to the primary mechanism of distillation: vapor-liquid equilibrium and mass transfer via phase change. This model, different from the differential model used previously (Hwang and Helfferich, 1988, 1989), will clearly demonstrate the distributed character of a stagewise process with many stages.

The governing equations of the stagewise model, written in terms of the liquid- and vapor-phase mole fractions, x and y, of the light component, are listed in Table 1. The discussion will focus on the responses to feed composition disturbances, but the composition responses to flow rate disturbances (e.g., of the feed, reflux, or reboil) also can be calculated by assuming that the internal flow rates respond virtually immediately compared with the slow composition responses. A normalized time τ is defined to cover various columns with different flow rates and holdups, as shown in Table 1, which also lists holdup parameters. The governing equations were converted to a set of pseudolinear finite-difference equations and then solved iteratively using the well-known tridiagonal algorithm. A similar technique was used to solve the steady-state version of the model.

With the assumptions mentioned above, the main source of nonlinearity in this model is the equilibrium relation. In this article, a binary mixture with a constant relative volatility $\alpha=2$ is chosen not only for simplicity but also for demonstrating that even such an ideal system in a simple column can exhibit severely nonlinear behavior. The equilibrium curve of this binary system is given in Figure 2.

For illustrating the limitation of conventional linearized models in describing the nonlinear behavior of high-purity columns, the stagewise model is linearized for the responses to feed composition disturbances, which are of major interest in this article. The linearized model is presented in the Appendix. One may expect that the limitation of this linearized stagewise model will also be applicable to linearized reduced-order models (by lumping stage compositions conceptually in various ways) commonly used for distillation control analysis and implementation.

Nonlinear Behavior of Rectifying Columns

To clarify the causes for dynamic effects, the rectifying column in Figure 1c and the fractionating column in Figure 1a will be discussed first. Included is a simple situation with a negligible condenser holdup, and thus a negligible reflux lag as well as the effect of the reflux lag. We will demonstrate the strong nonlinear behavior in a high-purity column vs. the nearly linear behavior in a low-purity column. (Although the term "high purity" for a rectifying column may not be as appro-

Table 2. Parameter Values of Example Distillation Columns

Binary Mixture	
Relative volatility	$\alpha = 2$
Rectifying Column	
Number of plates	$N = 40$ (high-purity column) $N = 10$ (low-purity column) $N = 20$
Reflux ratio	$R = 3$
Feed status	$q = 0$ (saturated vapor)
Feed concentration	$y_F = 0.50 \pm 0.05$
Vapor-to-liquid holdup ratio	$r = 0.01$
Normalized condenser holdup	$h_D = 0$, 2 (effect of reflux lag)
Fractionating Column	
Number of plates	$N = 50$
Feed plate location	$M = 26$
Reflux ratio	$R = 3$, 2.5 (min. reflux condition)
Reboil ratio	$S = 8/3$, 7/3 (min. reflux condition)
Feed status	$q = 1$ (saturated liquid)
Feed concentration	$x_F = 0.40 \pm 0.02$
Vapor-to-liquid holdup ratio	$r = 0.01$
Normalized reboiler holdup	$h_B = 0.1$, 2 (effect of reboil lag)
Normalized condenser holdup	$h_D = 0$

priate as for a fractionating column, it will be used here in a similar sense.) The parameter values of the example rectifying columns are given in Table 2.

Steady-state profiles

Figure 3a presents three nearly linear steady-state profiles (plotted as continuous curves for better visualization) in a low-purity column ($N = 10$); Figure 3b, strongly nonlinear profiles in a high-purity column ($N = 40$). The base case B (with $y_F = 0.50$) gives the maximum separation. For the 40-plate column, case A represents an under-reflux operation with respect to a feed of lower concentration; case C, an over-reflux situation, in which the separation is essentially completed in the bottom half of the column. An important character of such a high-purity column is that at least one end of the column is pinched; for the optimal steady state B, both column ends are pinched. The operating lines of the three steady states in the 40-plate column are plotted on Figure 2 along with the equilibrium curve.

The steady-state profiles in the two columns have quite different characters, especially for the transitions between steady states. In the transition from steady state B to A, the compositions on all plates change by nearly the same amount in the 10-plate column, but by extremely different amounts in the 40-plate one. From another point of view, the profile shifts only a short distance in the 10-plate column, but almost all the way to the top in the 40-plate column.

Steady-state gains

The sensitivity to disturbances of a process can be characterized by steady-state gains. By considering a step disturbance, a steady-state gain here is defined as the ratio of the final deviation of a state variable from its initial steady-state value to the input step change. The difference in the steady-state characters of the above two columns leads to drastically different behavior of steady-state gains with respect to their dependence on the magnitude and direction of the input step change. For the steady-state B, the gains at two locations are

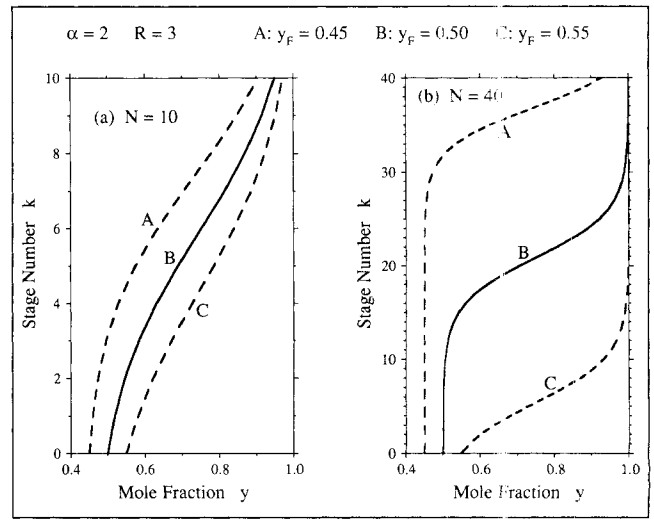

Figure 3. Steady-state profiles of rectifying columns.

a. Nearly linear profiles in 10-plate column; b. strongly nonlinear profiles in 40-plate column

of most interest: at the top of the column (distillate) and at the sharpest point of the steady-state profile (plate 6 of the 10-plate column and plate 21 of the 40-plate column). The latter is often suggested for the temperature sensor location (and thus as the control plate) to control a distillation column. Figures 4a and 4b present the compositions at these locations vs. the feed composition y_F. Figures 4c and 4d show the steady-state gains of theses compositions resulting from various feed concentration changes δy_F within ± 0.05 from $y_F^o = 0.5$; the gains at $\delta y_F = 0$ represent the values predicted by the linearized model using Eqs. A7 and A8 in the Appendix, and are listed in Table 3 along with the gains for several other plates.

At the top column end, the distillate composition on the 10-plate column has some room to respond to feed concentration changes in both directions while that in the 40-plate column

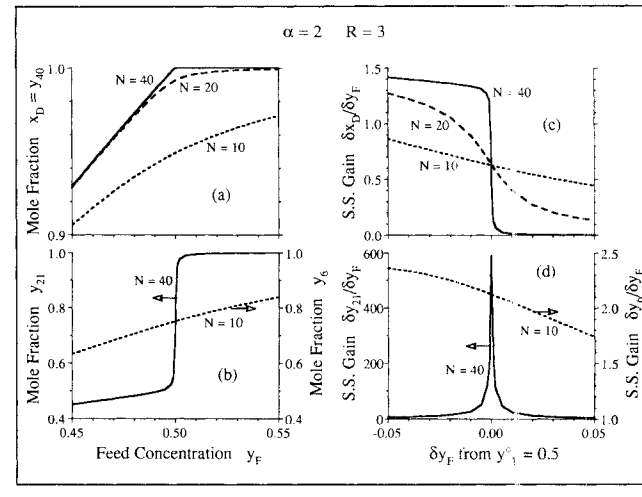

Figure 4. Dependence of compositions and steady-state gains on feed composition change in rectifying columns.

a, b. Compositions; c, d. steady-state gains

Table 3. Steady-State Gains, Limits of Disturbances, and Time Constants for Linearized Models of Example Distillation Columns

Rectifying Columns ($h_D = 0$): Steady State, $y_F^o = 0.5$

N	Stage k	Gain $\delta y_k/\delta y_F$	Limits* of δy_F	Mode j	Time Constant θ_j**
10	1	1.23	−0.095	1	4.57
	5	2.20	to	2	0.53
	6	2.13	+0.081	3	0.22
	20	0.63		.	.
20	1	1.26	−0.011		
	10	11.2	to		
	11	11.4	+0.012		
	20	0.64			
40	1	1.25	−0.00021	1	584
	20	573	to	2	0.70
	21	589	+0.00021	3	0.45
	22	559		.	.
	40	0.67		40	0.007

Fractionating Column ($h_B = 0.1$, $h_D = 0$): Steady state, $x_F^o = 0.4$

N	Stage k	Gain $\delta x_k/\delta x_F$	Limits* of δx_F	Mode j	Time Constant θ_j**
50	(Rb) 0	0.79	−0.00012	1	444
	1	1.36	to	2	0.82
	20	868	+0.00011	3	0.28
	21	917		4	0.16
	22	903		5	0.14
	(F) 26	459		6	0.095
	31	1458		.	.
	32	1510		.	.
	33	1442		50	0.002
	50	2.64		51	0.002
	(Cd)	1.32			

*Limits ensuring that all mole fractions at the final steady state are between 0 and 1, and monotonic with the stage number k.
**In decreasing order, θ_1 is the largest time constant.

has no room to respond to feed concentration increases since the top end is pinched. Consequently, the steady-state gain of the distillate composition in the 10-plate column depends weakly on the input step change (nearly linear behavior) while that in the 40-plate column varies drastically in a range of very small disturbances. Similar nonlinear behavior caused by such a no-room-for-response situation was observed by Weigand et al. (1972) in their numerical simulation of a fractionating column. The 20-plate column exemplifies a case between nearly linear and severely nonlinear behavior. At the sharpest point of the steady-state profile B, plate 6 of the 10-plate column behaves much like the top plate; in contrast, the behavior of plate 21 of the 40-plate column differs greatly from that of the top plate. For a very small step change of the feed composition in either direction, the steady-state gain of y_{21} is extremely large (the peak value at $\delta y_F = 0$ is calculated with the linearized model). Figure 4d demonstrates a strong dependency of the gain on the input step change δy_F from a fixed initial steady-state feed composition $y_F^o = 0.5$; this differs from the similar peak pattern presented earlier by Kapoor et al. (1986) for the dependence of a lumped gain on the steady-state feed composition (a counterpart of y_F^o here). The former reflects a typical nonlinear character, whereas the latter can result even from a linearized model.

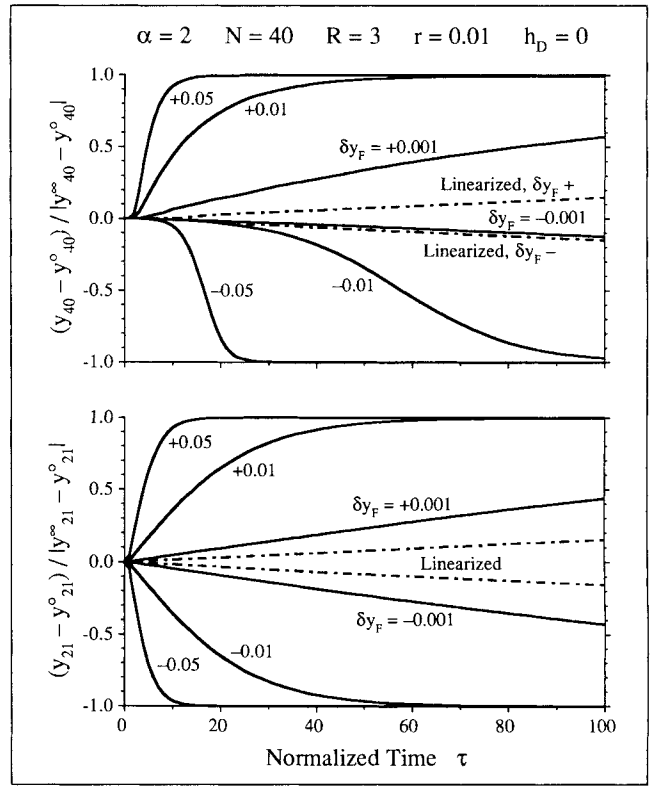

Figure 5. Strong dependence of response lags of compositions on magnitude of feed composition change in high-purity rectifying column.

Response of linearized model is included for comparison

Dynamics: response lags

Nonlinear behavior of a high-purity column is also reflected by the response lags (time constants of linear models) in addition to the gains. Figure 5 presents the response curves of the top plate and plate 21 of the 40-plate column at the steady state B in response to various step disturbances of different magnitudes and directions. These response curves show that a smaller disturbance leads to a more sluggish response. This agrees with the numerical simulation results of Luyben (1971) and of Fuentes and Luyben (1983) for high-purity fractionating columns.

For a comparison between the dynamic behavior predicted by the nonlinear simulation and by the linearized model, Figure 5 also includes the response curves resulting from the latter. For the linearized response (independent of the input step change), the largest three time constants (the same set of time constants applies to all plates) are listed in Table 3. The response curves in Figure 5 imply that, for a high-purity column, the linearized model is limited to a very narrow range of small disturbances, as will be discussed below.

Limitation of linearized model

In the conventional way of constructing a linearized dynamic model, small perturbations of state variables from an initial steady state are considered. For a reasonably good approximation, the perturbations must be small enough at all times,

and thus the linearized model is limited to sufficiently small disturbances. For the example rectifying columns in discussion, the limits of a step disturbance may be evaluated by requiring all final steady-state mole fractions being physically plausible ($0 \le y^{\infty}_k \le 1$ and monotonic with k). Following this criterion, Table 3 lists the limits of δy_F for the steady state B ($y^o_F = 0.5$) in 10-, 20- and 40-plate rectifying columns, respectively. Because the gains in the middle portion of the 40-plate column are very large (see Table 3), the linearized model for such a high-purity column is limited to extremely small disturbances. Moreover, these limits of δy_F ensure physically plausible compositions only, but not necessarily good predictions. A comparison of the gains of the linearized model (independent of δy_F) and those calculated with the nonlinear simulation (varying with δy_F) showed that the discrepancy is within $\pm 7\%$ for the 10-plate column with δy_F in the range of ± 0.01, but is as large as $\pm 20\%$ for the 40-plate column with δy_F even as small as ± 0.0001.

It becomes apparent that conventional linearized models, though having worked well for columns with products in low to moderate purity, are inadequate for high-purity columns in response to sustained disturbances such as step changes since the models are often limited to disturbances too small to be of practical interest. As a complement to conventional linearization, a better tool is needed to handle the nonlinear behavior of distillation columns more effectively.

Nonlinear Wave Theory

For the high-purity rectifying column with steady-state profiles shown in Figure 3b, one may imagine the movement of such a profile during a transition from one steady state to another as a traveling wave. The theory for such nonlinear wave behavior has been well developed for fixed-bed sorption (for reviews, see Glueckauf, 1955; Vermeulen, 1958; Helfferich, 1962; Vermeulen et al., 1984) and adapted to simple countercurrent separation processes previously (Hwang and Helfferich, 1988). A brief review of this theory will be given below, starting with an example of fixed-bed ion exchange. Ion exchange is selected because its equilibrium behavior is usually described in a way mathematically analogous to a vapor-liquid equilibrium relation for distillation.

Consider a binary ion-exchange system with two monovalent counterions (e.g., Na^+ and K^+) and choose x and y to denote the liquid- and exchanger-phase mole fractions, respectively, of the counterion with higher affinity to the exchanger (say, K^+). Binary ion-exchange equilibrium is usually described with a separation factor α, which is mathematically equivalent to a relative volatility for distillation.

Nonlinear waves in fixed beds

The differential material balance for ion exchange in a fixed bed is (axial dispersion by diffusion or hydrodynamic mixing is neglected; see Notation for symbols):

$$\frac{\partial x}{\partial t} + r\frac{\partial y}{\partial t} + v^o\frac{\partial x}{\partial z} = 0 \tag{1}$$

Assuming the liquid flow is so slow that local equilibrium is ideally attained, one may substitute y in Eq. 1 with the equilibrium relation. This leads to an equation for the "wave velocity" tracking the propagation of a specific value of concentration x:

$$v_x \equiv \left(\frac{\partial z}{\partial t}\right)_x = \frac{v^o}{1 + r(dy/dx)} \tag{2}$$

where dy/dx is the slope of the equilibrium curve at the specific value of x. This velocity is a "natural" velocity of the wave in the sense that it reflects the intrinsic behavior pertinent to the equilibrium between the two phases while disregarding the dissipative effects of nonequilibrium and dispersion.

As Eq. 2 indicates, the wave velocity varies with concentration for a system with nonlinear equilibrium, and therefore varies with location z within a wave. Consequently, a wave tends to sharpen if v_x decreases with z, and to spread if v_x increases with z; the former has been known as a "self-sharpening" wave and the latter, a "nonsharpening" wave. Under the hypothetical local equilibrium condition, a self-sharpening wave eventually becomes a discontinuity, of which the travel can be characterized by a "shock wave velocity" derived from a material balance across the wave:

$$v_\Delta \equiv \left(\frac{\partial z}{\partial t}\right)_\Delta = \frac{v^o}{1 + r(\Delta y/\Delta x)} \tag{3}$$

where Δ denotes the difference between the two sides of the shock wave (the two phases on each side of the wave are in equilibrium). In reality with dissipation, a self-sharpening wave eventually attains a "constant pattern" (with a fixed shape) as soon as its intrinsic sharpening tendency is balanced by the dissipative effects. Nevertheless, the travel of a constant-pattern wave obeys Eq. 3. For a nonsharpening wave, the dissipative effects eventually become insignificant compared with the intrinsic spreading effect.

Referring to the example mentioned above (K^+/Na^+) and assuming $\alpha = 2$ so that the equilibrium curve is the same as the one for distillation shown in Figure 2, consider a bed of exchangers completely loaded with K^+ ($y = 1$) and in equilibrium with a presaturant containing only the same counterion ($x = 1$); this condition is represented by point U in Figure 2. Then, a feed of composition indicated by point E is introduced to the bed with a downward flow rate L, as Figure 6Ia shows. Such a step change of liquid composition leads to a nonsharpening wave since the wave velocity increases from point E to U (following the equilibrium curve, the slope dy/dx decreases). After the bed has been completely saturated, the feed E is replaced by the presaturant U to regenerate the bed, as Figure 6Ib illustrates. This step change, in contrast, leads to a self-sharpening wave because the wave velocity decreases from point U to E. This wave soon becomes a constant-pattern wave traveling at a shock wave velocity expressed by Eq. 3 with $\Delta y/\Delta x$ being the slope of line UE in Figure 2. The calculation of this velocity needs the information only at points U and E on the two sides of the wave, and nothing in between.

Countercurrent processes: standing waves

The fixed bed of ion exchange can be converted to a countercurrent moving bed by continuously transporting the ex-

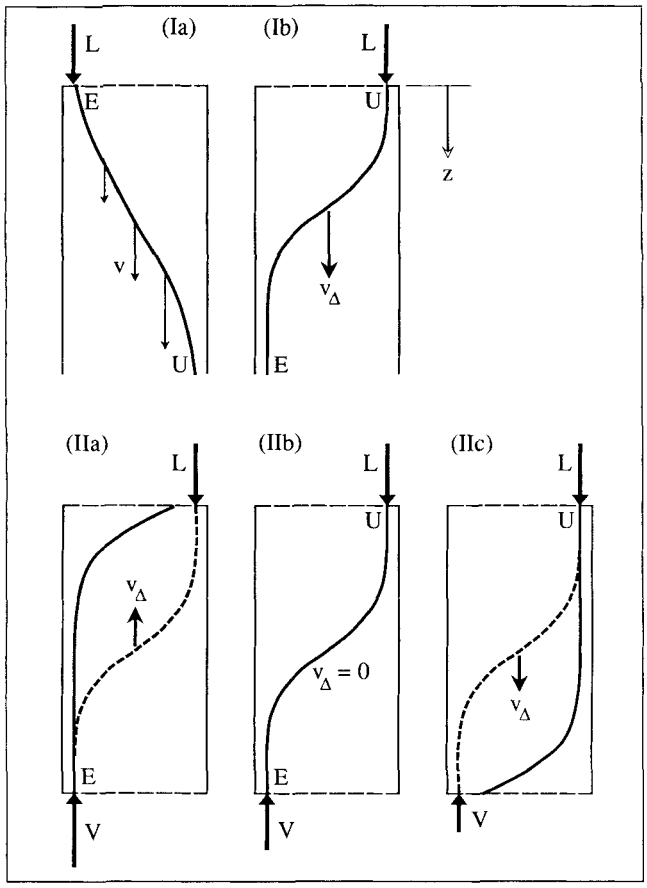

Figure 6. Nonlinear wave propagation.

Ia. Nonsharpening wave in fixed bed; Ib. self-sharpening wave in fixed bed; IIa-IIc. self-sharpening waves in countercurrent process.

changer phase upward with a supply of the same composition at a flow rate V, as illustrated by Figures 6IIa to 6IIc for the regeneration shown by Figure 6Ib. Assume that the column is long enough to contain the entire constant-pattern wave at the starting moment so that the two phases near both column ends are essentially in equilibrium (compositions U and E in Figure 2). The upward flow rate can be adjusted so that the wave becomes a "standing wave" (Hwang and Helfferich, 1988) with a *zero* shock wave velocity as demonstrated by Figure 6IIb. The result is a steady state which will be referred to as "balanced" in the sense that the convective transports of counterions by the two countercurrent streams are balanced. This steady state, which gives the maximum separation, can be represented by the operating line EU in Figure 2. If the upward flow rate is too low, the wave will still travel downward at a reduced velocity, as Figure 6IIc shows, until it approaches the bottom end of the column. At the end, the tendency of the wave to travel out of the column will lead to a nonequilibrium condition, which will then enhance the mass transfer between the two phases and thereby halt the wave. On the other hand, if the upward flow rate is too high, the wave will be pushed upward until it approaches the top end, at which it will be stopped by a similar nonequilibrium condition, as Figure 6IIa illustrates. Furthermore, even with a proper upward flow rate, if the concentration of the exchanger stream is either lower or higher (e.g., represented by point J or K in Figure 2) than that originally in the bed (point E), the result will be much the same as shown by either Figure 6IIa or 6IIc. In all cases, the self-sharpening nature of the wave will not be affected by the countercurrent stream.

The same scenario is performed in a packed gas absorber with the vapor phase playing the role of the exchanger phase in the above moving bed; this was analyzed in detail previously (Hwang and Helfferich, 1988). It has been well known that the overall column behavior of a plate column with many plates (typical for high-purity columns) is similar to that of a packed column. Based on this similarity, Gilles and Retzbach (1980, 1983) and Marquardt (1985, 1988) successfully approximated the behavior of plate distillation columns with models assuming a continuous character of the columns. Without considering the column-end effect, however, they offered little analysis of the intriguing nonlinear phenomena in discussion here because the end effect is an essential cause of these phenomena, as will be clarified in this article. Here, the nonlinear wave theory developed previously for packed gas absorbers (Hwang and Helfferich, 1988) will be applied to the example rectifying column, and the effect of reflux will be supplemented; such an application will be extended to the example fractionating column later.

Nonlinearity and high purity

The above example of ion exchange shows that the travel of a composition wave implies an imbalance of convective transports between the two phases in equilibrium (always so in a fixed bed). In a countercurrent process such as a rectifying column, the wave stands still at a steady state either because the convective transports are balanced by a deliberately maintained condition (the balanced steady state), or because the imbalance of convective transports is counteracted by the nonequilibrium condition established at a column end. For most binary distillation processes, the standing wave in a column (or a section) is self-sharpening since the corresponding portion of the equilibrium curve is as a whole concave toward the operating line, as Figure 2 illustrates. Moreover, it is obvious that the standing wave in a high-purity column is always self-sharpening since a nonsharpening wave would stretch to both column ends and leave no refining zones there. Focusing on high-purity columns, the discussion hereafter will consider only composition profiles with self-sharpening tendency (however, a disturbance wave traveling over a self-sharpening background may be nonsharpening, as will be exemplified later).

In a low-purity column (one with a nonsharpening wave, a column too short to contain an entire self-sharpening wave, or a process with linear equilibrium), the wave, which stretches to both ends, has little tendency to travel since nonequilibrium conditions are maintained at both column ends. As a result, the behavior of a low-purity column is fairly linear in the sense that a small disturbance leads to merely a small shift of the profile. In contrast, in a high-purity column, the self-sharpening wave, occupying only a small portion of the column, tends to travel to either column end unless the balance of convective transports is carefully maintained. Consequently, the behavior of a high-purity column is severely nonlinear since even a small upset of the balanced condition will result in a large shift of the profile. Thus, in addition to the nonlinearity

of the equilibrium relation, the high-purity condition also has a critical contribution to the nonlinearity of the column behavior. Such a cause of nonlinear behavior can be generalized to pinched conditions, covering those at the azeotropes of highly nonideal mixtures.

As an interpretation in terms of material transport, one may consider two mechanisms of transporting material from one end to the other through a continuous (e.g., packed) column for the desired separation. One is an equilibrium convection mechanism, which transports material through the column under the ideal condition of plug flow and local equilibrium between the two phases and is the intrinsic driving force for the nonlinear wave propagation; the other is a dissipation mechanism which transports material via axial dispersion/diffusion and "leaking" (material escaping from being captured by the other phase to attain equilibrium) owing to a finite transfer rate between the two phases. The same mechanisms apply as well to plate columns with many plates. Since the equilibrium relation is normally the major source of nonlinearity, the first mechanism is the primary cause of the nonlinear column behavior. In a low-purity column, a substantial part of material transport is via the dissipation mechanism because axial dispersion is relatively significant in a short column and "leaking" is intensified by the nonequilibrium conditions at the column ends. In contrast, in a high-purity column (long with pinched ends), the material transport relies mainly on the equilibrium convection mechanism, and thus the column exhibits strongly nonlinear behavior. Accordingly, conventional linearized models are suitable for low-purity columns, while the nonlinear wave theory offers a better description of high-purity columns.

Wave velocities for distillation columns

The key of the nonlinear wave theory is the *natural* wave velocity, which represents the relative convective transport at equilibrium. Dependent only on the vapor-liquid equilibrium, such a velocity in a plate column can be calculated as if the column were continuous (like a packed column). For this purpose, a continuous normalized distance, σ, from the bottom of the column is defined as the fraction of column length in terms of number of plates (see Table 1; note that σ is in the direction of the vapor stream and is opposite to the distance z used above for the fixed bed). In terms of the normalized time and distance, a differential material balance can be written for a section of a distillation column with flow rates L and V as follows:

$$\frac{\partial x}{\partial \tau}+r\frac{\partial y}{\partial \tau}-\left(\frac{L}{F}\right)\frac{\partial x}{\partial \sigma}+\left(\frac{V}{F}\right)\frac{\partial y}{\partial \sigma}=0 \tag{4}$$

Applying similar procedures as for deriving Eqs. 2 and 3 to Eq. 4 results in the following normalized wave velocities.

Normalized Wave Velocity:

$$u\equiv\left(\frac{\partial \sigma}{\partial \tau}\right)_{x \text{ or } y}=\left(\frac{V}{F}\right)\frac{dy/dx-L/V}{1+r(dy/dx)} \tag{5}$$

Normalized Shock Wave Velocity:

$$u_\Delta\equiv\left(\frac{\partial \sigma}{\partial \tau}\right)_\Delta=\left(\frac{V}{F}\right)\frac{\Delta y/\Delta x-L/V}{1+r(\Delta y/\Delta x)} \tag{6}$$

Note that the value of $u\Delta$ falls between those of u for the compositions on the two sides of the wave. The flow rate ratio in the rectifying section is related to the reflux ratio by $L/V=R/(R+1)$.

Nonlinear wave propagation

As mentioned earlier, self-sharpening waves are of major interest for high-purity columns. The propagation of such a wave during a dynamic response can be characterized simply by a shock wave velocity given by Eq. 6, and the entire response can be approximately predicted by the nonlinear wave theory. For example, consider a transition in the 40-plate rectifying column from steady state B to A shown in Figure 3b. The balanced standing wave of steady state B is associated with a zero shock wave velocity corresponding to the slope of the operating line EU ($\Delta y/\Delta x=L/V=0.75$) shown in Figure 2. The step change of the feed composition from E to J will lead to a disturbance wave, represented by line JE (a self-sharpening wave with $u_\Delta=0.41$ according to Eq. 6), traveling into the column. This disturbance wave will soon catch up and merge with the standing wave EU in the middle portion of the column (takes about 1.3 units of τ, estimated assuming that the disturbance wave would travel to plate 21 at a constant velocity $u_\Delta=0.41$) to result in a new self-sharpening wave, which can be represented by line JU (line not drawn in Figure 2, slope $\Delta y\Delta x=0.775$) since the distillate composition U will be preserved until this wave approaches the top end. According to Eq. 6, this resulting wave will travel upward at a velocity $u_\Delta=0.025$ until it approaches the top end and is halted there by a nonequilibrium condition (indicated by the shift of the distillate composition from U to U′). The final steady state A is represented by the operating line JU′ with a slope L/V. As a quick approximation, one may assume that the wave JU would travel from plate 21 (representing the location of the standing wave at steady state B) all the way to the top end (the wave will be stopped near the top end at steady state A) at a constant velocity $u_\Delta=0.025$; this predicts that the transition will take about 19 units of τ. Similarly, a step change of the feed composition from E to K will lead to a new wave traveling downward with a negative shock wave velocity corresponding to the slope of line KU (line not drawn in Figure 2). As the wave KU approaches the bottom end, it will be stopped by a nonequilibrium condition there and eventually establish the final steady state with the operating line K′U.

In addition to the wave velocity, it is more convenient to represent the location of such a constant-pattern wave with a single point corresponding to a representative concentration. For the balanced standing wave of steady state B in Figure 3b, the wave velocity u of a specific concentration within this wave can be calculated with Eq. 5 using the slope dy/dx along the equilibrium curve segment EZU in Figure 2. This gives a zero u at point Z($y_s=0.775$) since the tangent at Z is parallel with line EU ($dy/dx=L/V$) and nonzero wave velocities elsewhere heading toward the location of y_s. Thus, the concentration y_s (or the corresponding x_s in the same equilibrium stage) is a

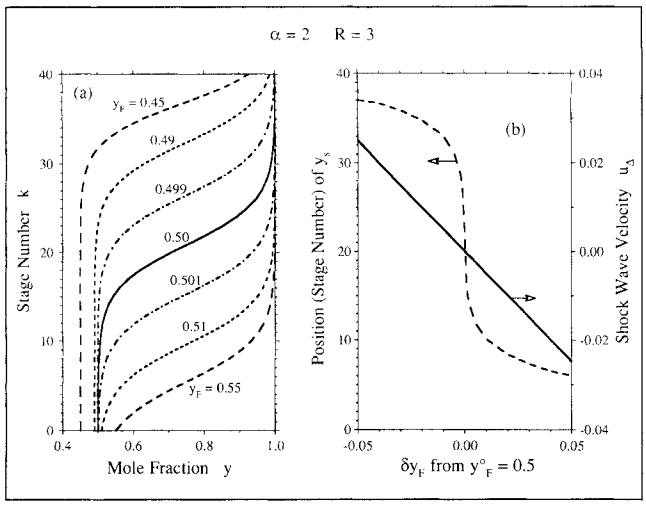

Figure 7. High sensitivity to disturbances of balanced steady state in high-purity rectifying column.

a. Shift of steady-state profile; b. distance (- - - -) and velocity (———) of profile shift

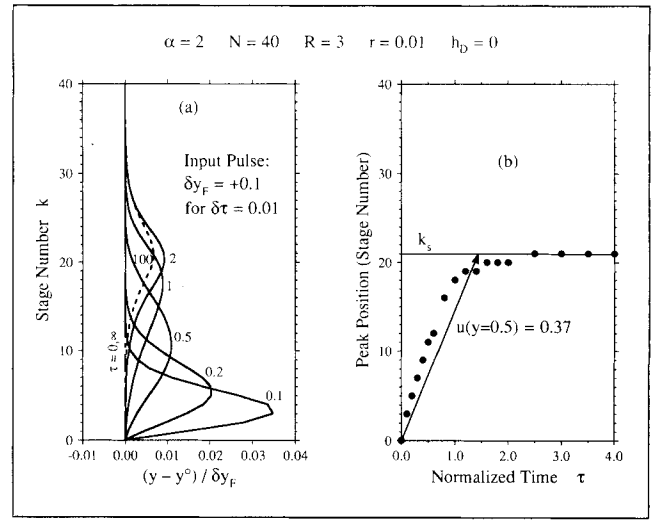

Figure 8. Propagation of pulse disturbance on steady-state background in rectifying column.

a. Transient profiles of pulse; b. trajectory of peak of pulse (arrow for approximation by nonlinear wave theory)

natural choice to represent the location of the standing wave; its corresponding position (plate number) k_s will be called the "stagnation point" (for $u=0$), same as that for a packed column discussed previously (Hwang and Helfferich, 1988). For the balanced steady state of the 40-plate column in discussion, k_s coincides with the sharpest point (plate 21) of the steady-state profile. The travel of the constant-pattern wave during a dynamic response can now be conveniently examined by tracking only the representative concentration y_s, instead of the entire wave.

Dynamics of Rectifying Columns

Steady-state gains and response lags

With the picture of nonlinear wave propagation, it is immediately clear that the balanced steady state of a high-purity rectifying column (e.g., B in Figure 3b) is extremely sensitive to perturbations. Any sustained disturbance such as a step change of either composition or flow rate of an entering stream will upset the balance of the convective transports and result in a wave with a nonzero velocity. Such a wave will travel outward until it approaches a column end. As a result, even a very small disturbance will lead to a considerable shift of the steady-state profile.

Figure 7a presents several steady-state profiles resulting from feed compositions slightly different from that (0.50) of the balanced steady state B shown in Figure 3b. The position of the representative concentration $y_s(0.775)$ vs. the feed concentration change δy_F from $y_F^\circ = 0.5$ is represented by the dashed curve in Figure 7b, which reflects that the gains of this steady state vary drastically in a range of very small perturbations as shown by Figures 4c and 4d. The way these gains vary can also be easily deduced from the shift of the steady-state profile shown in Figure 7a. The solid line in Figure 7b presents the normalized shock wave velocity of the wave resulting from a step change δy_F from $y_F^\circ = 0.5$; this relation is virtually linear within the range of interest. The two curves in Figure 7b reveal that, with a small change (say, -0.001) of y_F from 0.5, the profile needs to move a considerable distance (six plates up) with a very small wave velocity (almost zero). This explains why such a response is extremely sluggish and why a larger disturbance leads to a faster response, as shown by Figure 5.

The interpretation using the nonlinear wave theory clarifies the reason of high-purity columns having large time constants given by Skogestad and Morari (1987), whose explanation is that there is a large change in component holdup, but only a small imbalance to bring about the change. In terms of the wave concept here, once the balanced condition is perturbed, the wave will travel essentially all the way to one column end and thus will lead to a large change in component holdup, but the wave will travel only at a small velocity virtually proportional to the disturbance that created an imbalance of the convective transports by the two streams.

Propagation of disturbance pulses

The propagation of a disturbance pulse on the background of a steady-state profile was discussed in detail previously for packed gas absorbers (Hwang and Helfferich, 1988). The same approach can be applied as well to the rectifying column under discussion. As established previously, a small pulse disturbance travels at a velocity approximately the same as the natural wave velocity u for the background composition. The values of u along the profile of the balanced steady state B have been discussed earlier. Accordingly, a disturbance pulse introduced either to the feed or to the reflux (not usual in practice) will travel into the column, gradually slow down in the middle portion of the column, then become stagnant at the stagnation point k_s, and eventually die out there. Figure 8a confirms such a prediction by the wave theory with a numerical simulation result for a feed disturbance pulse of rectangular form with magnitude $\delta y_F = +0.1$ and duration $\delta\tau = 0.01$. Based on a differential model, Gould (1969) predicted the phenomenon of a pulse disturbance being trapped inside a distillation column with no discussion of the travel of the disturbance. The prop-

agation of a pulse can be simply represented by the trajectory of its peak, as the dots in Figure 8b illustrate. Such a trajectory can be approximately predicted in a simple way proposed previously. By approximating the sharp steady-state profile with two plateaus of the two column-end concentrations divided by a discontinuous step at the stagnation point k_s, one can view the disturbance pulse as if it traveled on a plateau of the feed concentration. Therefore, its trajectory can be established with a single wave velocity u for the feed concentration $y_F = 0.5$, as the arrow in Figure 8b illustrates.

As Figure 8a shows, the pulse takes about two normalized time units to reach the stagnation point $k_s = 21$, but diminishes very slowly, and much more slowly than a pulse in a gas absorber discussed in the previous study (Hwang and Helfferich, 1988). This reflects an effect of the reflux, which returns to the column a part of the perturbation leaving the top end and thus tends to keep the pulse inside the column. Later, the decay of such a pulse at a stagnation point will be discussed in more detail for a fractionating column.

Asymmetric dynamics

From computer simulations of fractionating columns, De Lorenzo et al. (1972) and Stathaki et al. (1985) concluded that a transition departing from the steady state with maximum separation is always faster than the return to it; moreover, Rose et al. (1956) and Mizuno et al. (1972) observed from their calculations that the difference in response times is usually drastic. Such asymmetric dynamics can be clearly explained using the nonlinear wave theory, as presented previously for a packed stripper (Hwang and Helfferich, 1989). Here, such a cause-and-effect analysis will be applied to the example rectifying column.

As discussed earlier, the transition from steady state B to A in Figure 3b is governed by the natural velocity ($u_\Delta = 0.025$) of the resulting self-sharpening wave JU (see Figure 2) until it approaches the top column end. Now, consider the return from steady state A to B initiated by changing the feed composition from J back to E shown in Figure 2. This step change will generate a disturbance wave EJ (a nonsharpening wave with u ranging from 0.37 to 0.45 according to Eq. 5) traveling on the background essentially of composition J, requiring about two units of τ to catch up and merge with the standing wave JU′ near the top end. The resulting wave EU′ will move downward quickly and thereby make the distillate concentration increase from U′ to U; this will soon lead to a new self-sharpening wave EU with *zero* shock wave velocity, which will have no intrinsic tendency to move further toward the middle portion of the column. The dissipative column-end effect, now no longer compensated by an outward natural wave velocity, will drive the wave inward. However, this effect decreases rapidly with the distance from the column end, so that the balanced wave will move more and more slowly toward its eventual steady-state location.

Referring to the two mechanisms of material transport discussed earlier, the dissipation mechanism is pretty weak in a high-purity column. For the transition departing from the balanced steady state, the disturbance creates an imbalance of the equilibrium convective transport and makes the equilibrium convection mechanism the principal driving force for this transition. In contrast, in the returning transition, the equilibrium convection mechanism is disabled by the restoration of the

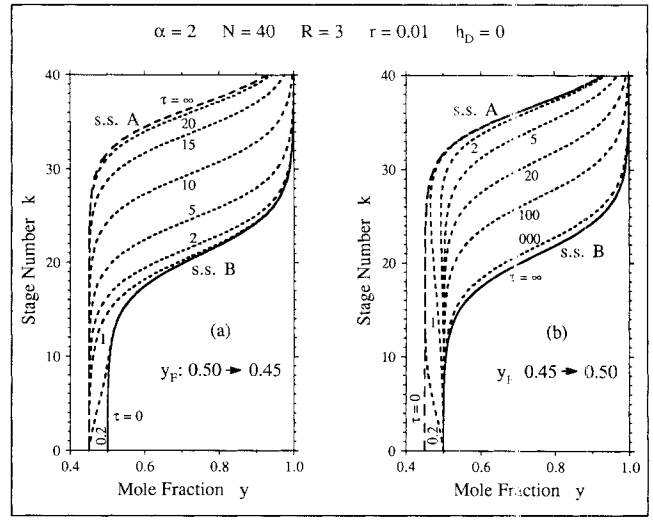

Figure 9. Asymmetric dynamics of rectifying column illustrated by transient profiles.

a. Transition departing from balanced steady state as a traveling wave; b. very slow returning transition with zero wave velocity

balanced condition and therefore leaves the weak dissipation mechanism as the only driving force. Without an intrinsic driving force, the return to the balanced steady state is naturally much slower than the departing transition.

Figures 9a and 9b present the transient profiles of the forward and returning transitions between steady states B and A. In the transition departing from the balanced steady state B shown by Figure 9a, the transient profile at $\tau = 0.2$ illustrates the disturbance wave JE (see Figure 2) on its way to merge with the standing wave EU; that at $\tau = 1$, the resulting wave JU. The transient profiles from $\tau = 1$ to 15 reveals that the resulting wave JU travels at a constant shock wave velocity. As Figure 9a shows, the quick approximation mentioned earlier (that the transition takes 19 units of τ) based on the natural wave velocity ($u_\Delta = 0.025$) of the wave JU is fairly close. In contrast to this transition, which is virtually complete in merely 25 units of τ, Figure 9b illustrates the much slower return, which takes more than 1,000 units of τ. Figure 9b also demonstrates the slowing down of the balanced wave EU on its travel. So far, a sufficiently simple approximation to predict the slow returning transition quantitatively has not yet been established.

Effects of reflux

As mentioned earlier, the reflux tends to keep a pulse disturbance inside the column by returning part of it back to the column. Since the pulse will linger for a very long time, such an effect may be cumulative if subsequent disturbances are mostly in the same direction.

For the responses to step disturbances, numerical computations have not turned up any significant difference in dynamics between the example rectifying column and a gas absorber (no reflux) investigated previously (Hwang and Helfferich, 1988) if the former has a condenser with a negligible holdup. If the condenser (including an accumulator or reflux drum) has a considerable holdup, it will obviously add a re-

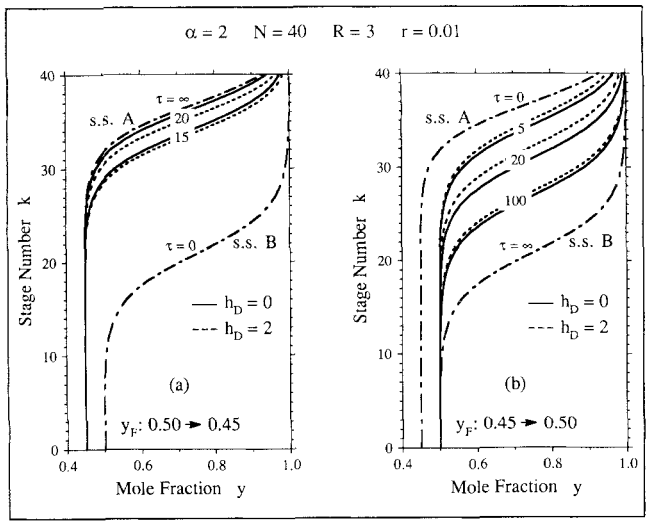

Figure 10. Minor effect of reflux lag on dynamics of rectifying column resulting from large condenser holdup.

a. In transition departing from balanced steady state; b. in returning transition

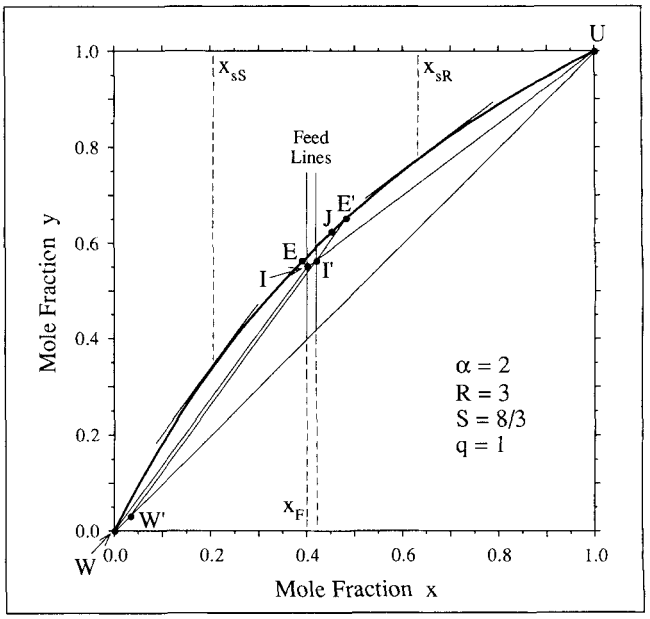

Figure 11. Operating lines of binary fractionating column and composition points showing nonlinear wave theory.

sponse lag to the entire process. With a condenser holdup twice as large as the total liquid holdup of the entire column, Figures 10a and 10b illustrate such an additional lag in the forward and returning transitions, respectively, between steady states B and A. For the transition from steady state B to A, the reflux lag has little effect until the wave approaches the top end and thereby starts to change the distillate composition (the transient profiles before $\tau = 15$ are virtually the same as shown in Figure 9a). For the returning transition, the reflux lag appears as soon as the balanced wave is generated and grows as the wave is pushed toward the middle portion of the column; the lag, however, diminishes when the wave moves further and the top end is pinched. This example demonstrates that, even if the condenser has a large holdup, the reflux lag has only a minor effect on the dynamic behavior of a high-purity rectifying column. The reason is that the factor dictating a composition response lag is actually the potential of change in component holdup, rather than the bulk holdup. Since a high-purity column tends to have a large change in component holdup in the column itself (the wave tends to travel all the way to one end), the change of component holdup in the condenser is often relatively small even though its bulk holdup may be larger than that of the entire column.

Fractionating Columns

In this section, the concept of nonlinear wave propagation will be extended to high-purity fractionating columns. The discussion will consider the example shown by Figure 1a with the parameter values listed in Table 2. The concepts demonstrated by the simple example can be applied as well to more complex columns.

Steady-state profiles

For the base case with $x_F = 0.40$, the given condition of flow rates leads to a desirable steady state producing both overhead and bottom products in high purity. For this steady state, lines WI and IU in Figure 11 represent the operating lines of the stripping and rectifying sections, respectively. Also, curve B in Figure 12 illustrates the steady-state profile in terms of the

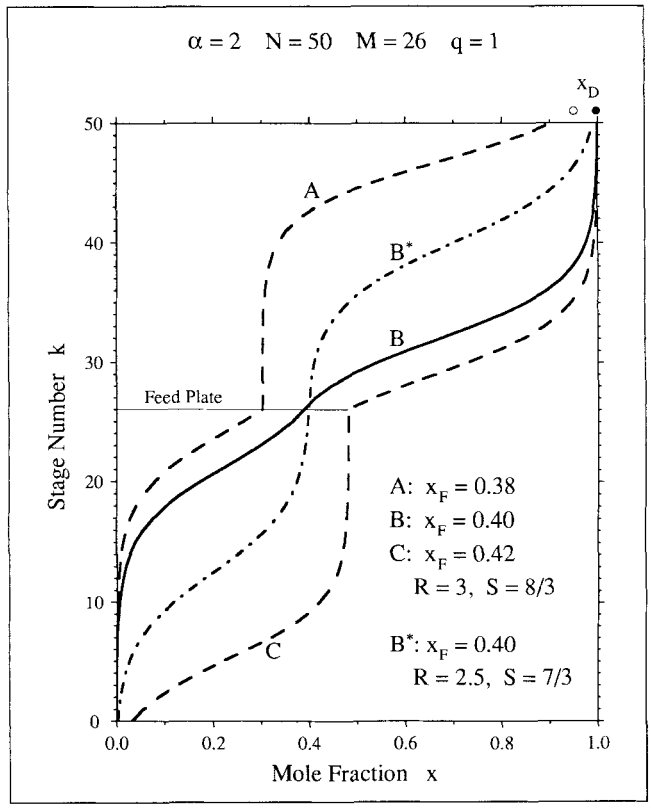

Figure 12. Steady-state profiles in fractionating column with different feed compositions and reflux and reboil ratios

liquid mole fraction; the profile reveals that plate 26 is the optimum feed-plate location for this operating condition. The composition on the feed plate is indicated by point E in Figure 11. As for the rectifying column discussed above, the portion of the steady-state profile in each section of the fractionating column can be characterized by a stagnation point. The stagnation point of the stripping section is plate 21, corresponding to $x_{sS}=0.206$ (see Figure 11); that of the rectifying section is plate 32, corresponding to $x_{sR}=0.633$. Each stagnation point coincides with the sharpest point of the profile in the respective section. With all other conditions fixed, a feed of higher concentration, $x_F=0.42$, will result in a steady state with a bottom product of lower purity ($x_B=0.033$) as illustrated by the operating lines W′I′ and I′U in Figure 11 and profile C in Figure 12. Likewise, a feed of lower concentration, $x_F=0.38$, will lead to a steady state with a lower-purity distillate, as profile A in Figure 12 shows.

For a fractionating column with a given feed, optimal separation conditions (with different levels of product purity) may result from an infinite number of pairs of reflux and reboil ratios. Referring to Figure 11, with points W and U virtually fixed (actually shifted within very small composition ranges) for the base case, point I will move along the feed line ($x_F=0.4$) if both R and S are changed properly. As point I approaches the equilibrium curve, the standing wave in each section approaches the character of a balanced wave (balanced within each section), as profile B* in Figure 12 illustrates. This minimum-reflux condition provides not only a limit of the operating condition, but also a criterion for a desirable steady state producing both products in high purity. This criterion says that the profile of such a dual high-purity steady state consists of a stripping-section profile above profile B* and a rectifying-section profile below profile B*, as exemplified by profile B in Figure 12. With the profiles in both sections squeezed toward the feed plate, only the small portion of the column around the feed plate is utilized for the major separation while the large parts toward both column ends are used for refining both products. At such a steady state, the convective transports by the three entering streams and the two leaving streams are balanced with respect to the vapor-liquid equilibrium.

Steady-state gains

Figures 13a and 13b present the compositions of the bottoms and the distillate as well as at the stagnation points for steady states with various feed concentrations around the base case $x_F=0.4$. Figures 13c and 13d show the steady-state gains of these compositions resulting from various step changes δx_F from $x_F^o=0.4$; the gains at $\delta x_F=0$ (e.g., the peak in Figure 13d) are obtained using Eq. A7 of the linearized model and are listed in Table 3. The balanced steady state B is extremely sensitive to both magnitude and direction of the disturbance. These patterns are similar to their counterparts shown in Figures 4a to 4d for the example rectifying column. The nonlinear behavior of steady-state gains in the fractionating column can be explained with the nonlinear wave concept as discussed earlier for the rectifying column. The wave propagation behavior of fractionating columns will be discussed below.

Wave velocities

As mentioned earlier, the key of the nonlinear wave theory

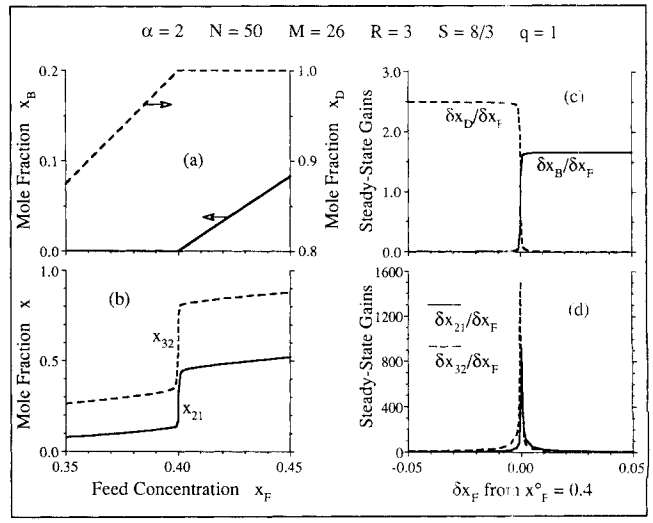

Figure 13. Strong dependence of compositions and steady-state gains on feed composition change in high-purity fractionating column.

a, b. Compositions; c, d. steady-state gains

is the natural wave velocity. The normalized wave velocities given by Eqs. 5 and 6 are applicable to any section of a distillation column with L and V representing the liquid and vapor flow rates, respectively, in that section. For the stripping section with flow rates $\overline{L}$ and $\overline{V}$, a slightly rearranged form is more convenient.

Normalized Wave Velocity:

$$u=\left(\frac{\overline{L}}{\overline{F}}\right)\frac{(\overline{V}/\overline{L})\,(dy/dx)-1}{1+r(dy/dx)} \tag{7}$$

Normalized Shock Wave Velocity:

$$u_\Delta=\left(\frac{\overline{L}}{\overline{F}}\right)\frac{(\overline{V}/\overline{L})\,(\Delta y/\Delta x)-1}{1+r(\Delta y/\Delta x)} \tag{8}$$

where the flow rate ratio is related to the reboil ratio by $\overline{V}/\overline{L}=S/(S+1)$

Propagation of disturbance pulses

As in a rectifying column, a small pulse disturbance introduced to the feed will travel essentially at the wave velocity for the background steady-state composition. For the steady state B shown in Figure 12, Eq. 7 for the stripping section gives a zero wave velocity u at plate 21 and nonzero wave velocities elsewhere heading toward this stagnation point; similarly, Eq. 5 for the rectifying section gives a zero u at plate 32 and nonzero velocities elsewhere heading toward plate 32. Accordingly, a small pulse disturbance of the feed composition will split into two response pulses, each traveling into one section shortly, becoming stagnant at the stagnation point of that section, and diminishing slowly there. Figure 14 confirms this qualitative prediction by the wave theory with a numerical simulation result for a rectangular disturbance pulse of magnitude $\delta x_F=+0.1$ and duration $\delta\tau=0.01$ (the two resulting pulses reach the stagnation points by $\tau=1$ as shown by solid

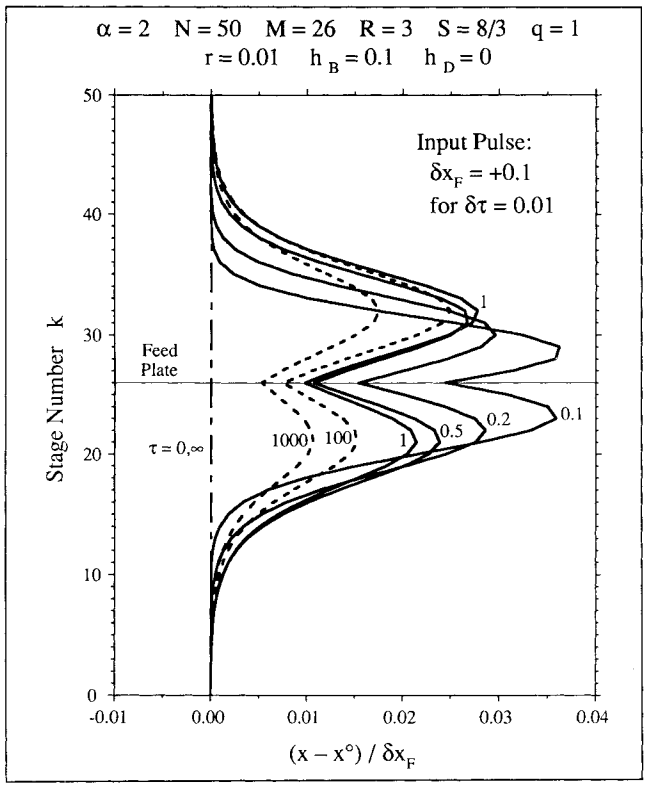

Figure 14. Propagation of pulse disturbance on steady-state background in fractionating column.

Short travel (———); slow diminishment at stagnation points (- - - -)

curves). As in a rectifying column, these pulses linger for a very long time (illustrated by dashed curves) owing to the effects of the reflux and the reboil. Apparently, such a persistent effect in a fractionating column lasts even longer since both leaving streams, only by which the perturbation can be relieved, are partially returned to the column.

The decay of the response pulses at the respective stagnation points can be measured in terms of the change in component holdup of the entire distillation unit including the reboiler and the condenser. A normalized total holdup of the light component can be defined as follows:

$$w \equiv h_B x_B + \frac{1}{N}\left(\sum_{k=1}^{N} x_k + r\sum_{k=1}^{N} y_k\right) + h_D x_D \qquad (9)$$

For the response pulses shown in Figure 14, the integral of a transient profile constitutes the major part of the deviation of w from its initial steady-state value. In the response to a small pulse disturbance, all compositions at all times are close to those at the initial steady state. Therefore, a linearized model may be applicable to such a situation. As discussed in the Appendix, the decay of the response pulses in the above example may be approximated by an exponential decay with a time constant $\theta_1 = 444$ (see Table 3). A comparison with the nonlinear simulation result showed that the approximation worked well for early transient behavior (within 5% error for $\tau \leq 100$), but gave a higher decay rate at later times (at $\tau = 1{,}000$, it predicted 11% of the input pulse remaining in the unit in contrast to 57% resulting from the nonlinear simulation).

Nonlinear wave propagation

At a balanced steady state of a fractionating column (e.g., B in Figure 12), the convective transports by three entering and two leaving streams are balanced with respect to the vapor-liquid equilibrium, as mentioned above. Any sustained disturbance (e.g., a step change) of either composition or flow rate of any entering stream will break the balance. The disturbance generates response waves that will quickly travel to and merge with the standing waves of the initial steady state. The resulting waves will still be self-sharpening, but now have nonzero natural velocities and so will move toward either end of their sections, downward if the feed concentration is increased and upward if it is decreased. The interaction between the two sections, however, complicates the picture. To calculate the natural velocity of the resulting self-sharpening wave in each section, one needs to identify the compositions on both sides of the wave. A key composition is on the feed plate, which is the junction of the two sections.

Consider the column at the steady state B (with $x_F = 0.40$) perturbed by a feed concentration increase (say, to 0.42). Such a step change will upset the balance of convective transports and lead to waves which tend to travel downward in both sections. In the rectifying section, the profile is already in the bottom portion and thus little change will occur. In the stripping section, in contrast, the profile has ample room to move toward the bottom end. The compositions on both sides of this traveling wave can be deduced backward from the steady state that will be established eventually (steady state C in Figure 12). Since a wave travels essentially at a constant velocity until it approaches a section end, the resulting wave will travel downward virtually all the way to the bottom end, regardless of the magnitude of the feed composition change (as long as it is not extremely small; very small perturbations are of little practical interest). Consequently, the top end (feed plate) of the stripping section will be pinched at the eventual steady state (this can also be reasoned from the fact that only a small portion of the section is responsible for the major separation). This implies that the new feed-plate composition can be identified at the intersection of the equilibrium curve and the new operating line of the stripping section, as exemplified by point E′($x_M = 0.482$) in Figure 11 for the eventual steady state C (with stripping line W′E′). The new feed-plate composition will be established at the moment the wave is formed; at that moment, the bottoms composition W will still be preserved until the wave approaches the bottom end. Accordingly, in terms of the compositions on its two sides, the resulting self-sharpening wave can be represented by line E′W (line not drawn in Figure 11), of which the slope ($\Delta y/\Delta x = 1.35$) is smaller than $\overline{L}/\overline{V}$ (1.375, slope of WI and W′E′). Calculated with Eq. 8, the normalized shock wave velocity of this wave is $u_\Delta = -0.041$. In a similar way, one can predict the response of the balanced steady state to a feed concentration decrease by focusing on the wave propagation in the rectifying section.

Figure 15 demonstrates the wave propagation behavior during the transition from steady state B to C. By assuming that the wave in the stripping section would travel all the way (21 plates, or 0.42 units of σ) down to the bottom end at a constant velocity $u_\Delta = -0.041$, one can approximately predict that this transition will take about 10 units of τ. As Figure 15 shows, it actually takes a longer time because the wave is gradually formed at the beginning and slows down when it approaches

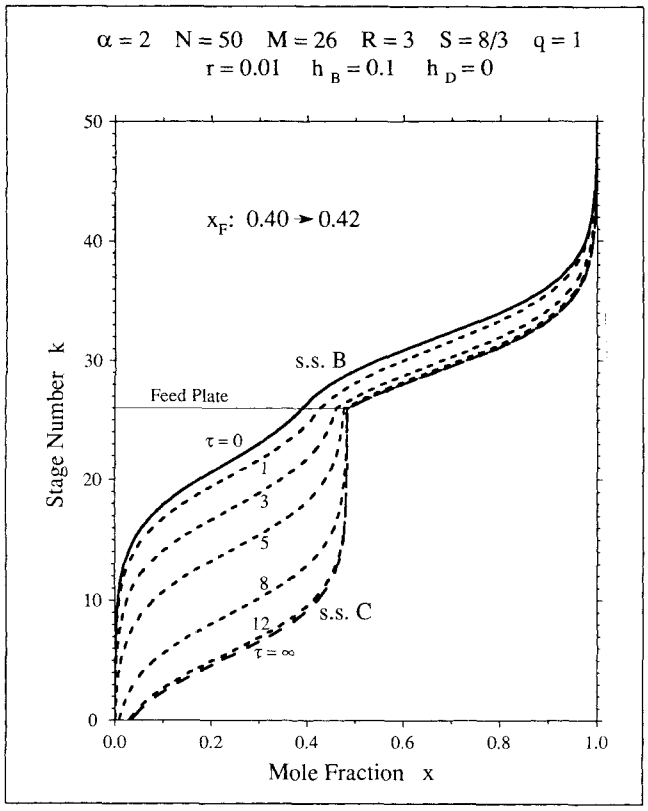

Figure 15. Nonlinear wave behavior of fractionating column during transition departing from balanced steady state.

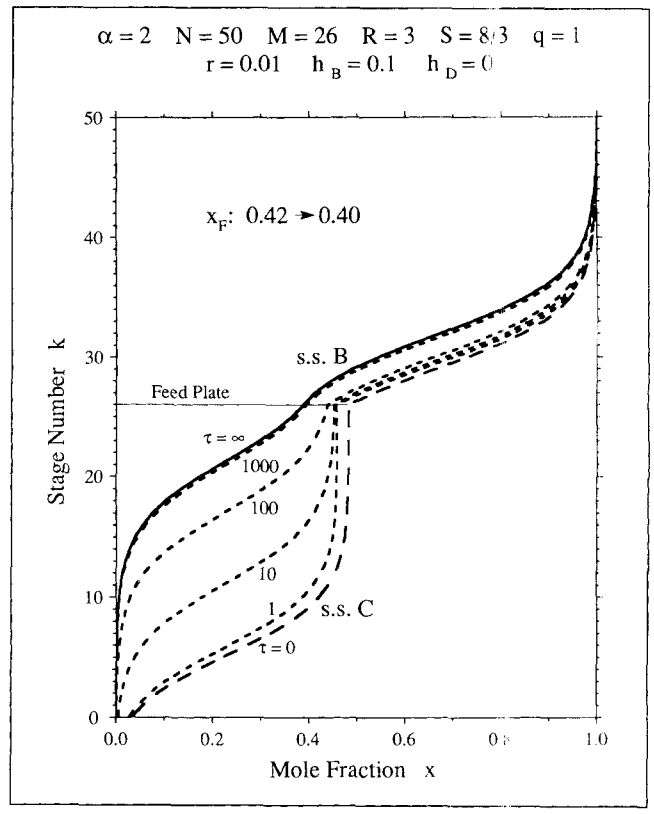

Figure 16. Asymmetric dynamics of fractionating column shown by slow return to balanced steady state driven by dissipative column-end effect alone.

the bottom end. From the standpoint of control applications, the dynamic information of most interest is that after the wave is formed (then the decrease of the product purity becomes noticeable) and before it approaches the column end. In such a highly interested zone, fortunately the nonlinear wave theory provides its best prediction of the wave propagation dynamics.

Asymmetric dynamics

In a previous section, the nonlinear wave theory provided a clear explanation for the asymmetric dynamic behavior of a rectifying column. Here, such a cause-and-effect analysis is to be expanded to fractionating columns.

Consider the returning transition from steady state C back to B initiated by a decrease of the feed concentration x_F from 0.42 back to 0.40. As before, the transient behavior in the rectifying section is of little importance. For the wave propagation in the stripping section, the feed plate plays a critical role. At the steady state C, the feed plate is under a pinched condition with composition E′ shown in Figure 11. The composition E′ will be reduced to a point J, an unknown composition to be identified, immediately after the feed composition is changed. The concentration decrease will lead to a disturbance wave JE′, which will travel downward and soon merge with the standing wave E′W′ near the bottom end. The merger will generate a wave JW′, which will move upward quickly and make the bottoms concentration decrease from W′ to W; this will result in a new self-sharpening wave JW. Since the feed plate will still be pinched at that moment, point J should be on both the equilibrium curve and the extension of the new stripping line WI for the eventual steady state B, as shown in Figure 11 ($x_M = 0.455$ at J). As a result, the new wave JW will have a *zero* shock wave velocity ($\Delta y/\Delta x = \bar{L}/\bar{V}$) and thus have no tendency to travel further toward the feed plate. The wave, however, will be pushed slowly away from the bottom end by the dissipative column-end effect as discussed earlier for the rectifying column. The wave will move more and more slowly since the dissipative effect will become weaker and weaker toward the feed plate. When the wave eventually approaches the feed plate, it will join with the wave in the rectifying section. The joined wave will be pushed upward very slowly since the convective transports are balanced in the entire column. The feed-plate concentration will decrease gradually from J to E and the steady state B will finally be established. Figure 16 presents the numerical simulation result of the slow return to the balanced steady state B; this result confirms the qualitative picture portrayed by the nonlinear wave theory. As mentioned earlier, a simple quantitative approximation has not yet been accomplished.

Figure 17 shows the response curves of the bottom product composition, the feed-plate composition, and compositions at the stagnation points (plates 21 and 32) during the forward and returning transitions between steady states B and C. For the slow return to the balanced steady state B, as the dashed curves illustrate, the responses on plates in the middle portion of the column are much more sluggish than that at the bottom end (reboiler), because the bottoms concentration decreases

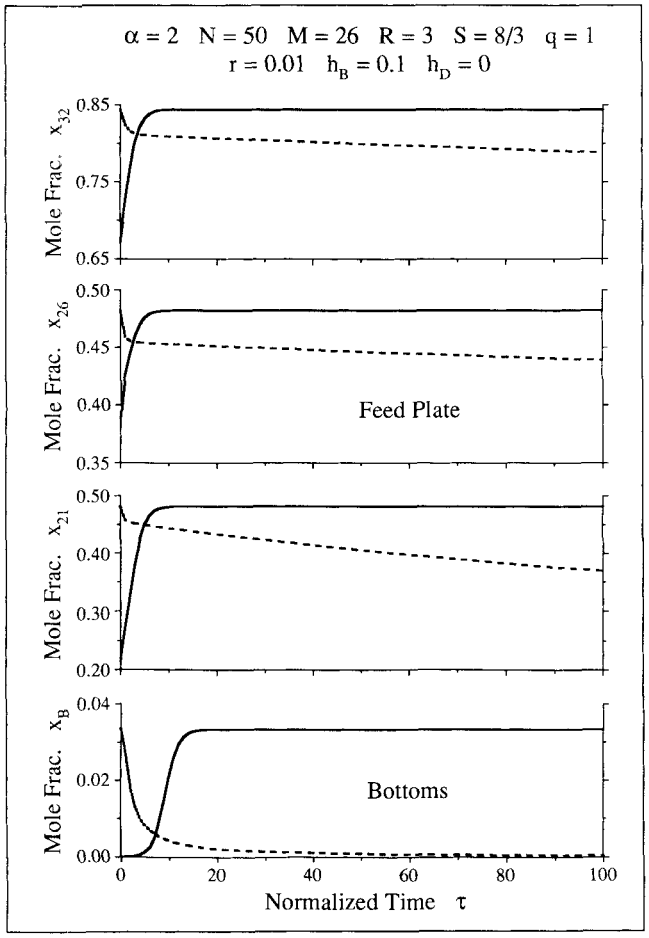

Figure 17. Asymmetric dynamics of fractionating column shown by response curves of compositions at bottom end, feed plate, and stagnation points.

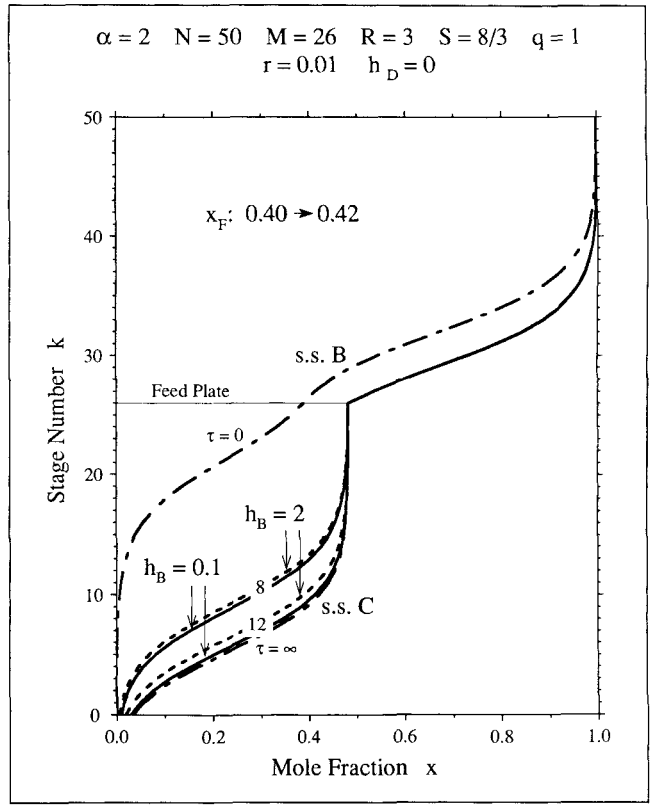

Figure 18. Minor effect of reboil lag on dynamics of stripping section of fractionating column resulting from large reboiler holdup.

rapidly from W′ to W before the zero-velocity wave JW is formed. This implies that a sensor at the bottom end tends to give a premature signal, and therefore, the return to the desirable steady state may tend to be incomplete, that is, the profile may tend to be closer than desirable to the bottom end (Hwang and Helfferich, 1989).

Start-up

During the start-up of a distillation column, the flow rates normally attain a steady-state condition much sooner than the compositions. After the establishment of the steady-state flow rates, the principal column dynamics can be analyzed with the same nonlinear wave concept as for the transitions between steady states. Thus, one can expect that the establishment of a balanced steady state will be much slower than that of an unbalanced steady state (with a low-purity product at one end) if no special maneuver is practiced, since the former involves the slow movement of a balanced wave driven by the column-end dissipative effect alone as in the return to a balanced steady state. Utilizing the wave theory, fortunately one can formulate an open-loop control strategy to accelerate such a start-up, as will be discussed later.

Effects of reflux and reboil

The dynamic effect of the reflux on a fractionating column can be expected to be much the same as that on a rectifying column discussed in a previous section. With both reflux and reboil, a fractionating column tends to keep short-duration disturbances such as pulses inside the column even longer, as mentioned earlier.

For the response to a sustained disturbance such as a step change, the reboiler will add a response lag to the dynamics of the entire column similar to the reflux lag if the reboiler has a considerable holdup. With a reboiler holdup twice as large as the total liquid holdup of the column, Figure 18 shows the reboil lag in the transition from steady state B to C illustrated by Figure 15. The reboil lag has little effect on the column dynamics until the wave approaches the bottom end and starts to change the bottoms composition (the transient profiles before $\tau = 8$ are essentially the same as shown in Figure 15). The reason why the reboil lag is usually insignificant to the column dynamics is the same as for the reflux lag discussed earlier. In summary, for a high-purity fractionating column, the reboil and reflux lags have effects on the wave propagation dynamics only in the vicinities of the column ends and therefore are unimportant to a control system of which the objective is to keep the profile in the middle portion of the column.

Ideas on control applications

Detailed discussions of applications of the nonlinear wave theory to distillation control are beyond the scope of this ar-

ticle, but some ideas on such applications are proposed here to briefly illustrate the anticipated usage of this tool.

First, as proposed in a previous note (Hwang and Helfferich, 1989), one can exercise a two-step open-loop maneuver to greatly accelerate the return to a balanced steady state or, more importantly, the start-up establishing such a steady state. In the first step, the control flow rate is overadjusted to generate a wave traveling at a nonzero velocity toward the feed plate; the time needed for such a wave to reach its target location can be estimated from its shock wave velocity. Then, when the estimated time has elapsed, the control flow rate is adjusted back to that for the balanced steady state.

For feedback control of a high-purity column, this nonlinear wave approach offers a handy tool for analyzing the profile-position control strategy pioneered by Luyben (1972) and later advanced by Gilles and Retzbach (1980, 1983). Also, this theory may be helpful in the implementation and analysis of dual-composition control by providing a quick way to deduce the response of the product compositions to a composition or flow change of any entering stream. In addition, the nonlinear wave concept may be used to develop a simple model for model-based control, as Marquardt (1985, 1988) did earlier (but ignoring the column-end effect).

Another possible application is the implementation of feedforward control. The nonlinear wave theory can satisfactorily predict the dynamic behavior of major interest to the control purpose with fairly simple mathematics, even for a mixture with a complicated vapor-liquid equilibrium relation. Therefore, one may use this theory to formulate feedforward control algorithms.

Conclusions

This study has developed a nonlinear wave theory for the nonlinear and distributed dynamics of binary distillation columns, with emphasis on columns producing high-purity products. This theory is an extension of a previous development (Hwang, 1987; Hwang and Helfferich, 1988, 1989), which adapted well-advanced theories of fixed-bed sorption to simple countercurrent separation processes. The extension includes in column dynamics the effects of reflux, reboil, and most importantly, combination of rectifying and stripping sections.

The nonlinear wave theory views the movement of sharp profiles in high-purity distillation columns as nonlinear waves. For most situations of interest, waves in distillation columns tend to sharpen and thereby become constant-pattern waves (with fixed shapes) as soon as their intrinsic sharpening tendency is balanced by the dissipative effects of nonequilibrium and dispersion. The travel of such a constant-pattern wave can be characterized by a shock wave velocity. With the compositions and flow rates of all streams entering a column deliberately manipulated to balance the convective transports with respect to the vapor-liquid equilibrium, one can maintain a standing wave with zero shock wave velocity in the middle portion of the column, thus leaving the large parts toward both column ends for refining both products. This balanced condition leads to a desirable steady state with both products in high purity. However, such a balanced steady state is by nature very sensitive to disturbances because any sustained disturbance (e.g., a step change) will upset the balance of convective transports and result in a new wave that will travel toward a column end with a nonzero velocity until halted by the boundary condition externally imposed on that end. Furthermore, the return to the balanced steady state by eliminating the disturbance will be very sluggish since the restoration of the balanced condition will lead to a wave of zero velocity, which will have to be pushed back to the middle portion of the column by the dissipative column-end effect alone.

This picture of nonlinear waves clearly elucidates the intriguing nonlinear phenomena observed by earlier investigators in their computer simulations, such as high steady-state gains, large response lags, strong dependence of dynamics on both magnitudes and directions of disturbances, and asymmetric dynamics of the transitions between two steady states. It also illuminates the reason why conventional linearized models are inadequate for high-purity distillation columns in response to sustained disturbances. The key of the nonlinear wave theory is the *natural* wave velocity representing the relative convective transport at equilibrium (regardless of the dissipative effects). Especially, the shock wave velocities of self-sharpening waves play the major role in nonlinear distillation dynamics. The calculation of a shock wave velocity requires only the equilibrium compositions on the two sides of the wave, but nothing in between, and the ratios of the flow rates as well as the holdups of the two phases. With such simple mathematics, the nonlinear wave theory provides a clear picture and a satisfactory prediction of the nonlinear dynamics of distillation columns. Applied to high-purity distillation columns, this theory may be useful for development of dynamic models, design of control systems, implementation of dual-composition control, and formulation of feedforward of other predictive control algorithms.

Acknowledgment

The author is very grateful to Prof. F. G. Helfferich of The Pennsylvania State University for his careful review of the draft with valuable suggestions, to Dr. G. E. Keller of Union Carbide Corporation for his encouragement of this study and his review of the manuscript, and to Prof. J. C. Friedly of the University of Rochester for his greatly helpful comments on the manuscript.

Notation

B = molar flow rate of bottom product, mol/s; as subscript, bottom product or reboiler
b_M = coefficient for feed composition disturbance of linearized model, see Eq. A5
c_k = kth subdiagonal element of tridiagonal coefficient matrix of linearized model, see Eq. A4
D = molar flow rate of distillate product, mol/s; as subscript, distillate product or condenser
d_k = kth diagonal element of tridiagonal coefficient matrix of linearized model, see Eq. A4
e_k = kth superdiagonal element of tridiagonal coefficient matrix of linearized model, see Eq. A4
F = molar flow rate of feed mol/s; as subscript, feed
f = function representing vapor-liquid equilibrium: $y=f(x)$
f' = derivative of function f with respect to x
G = molar vapor holdup of plate, mol
H = molar liquid holdup of plate, mol
H_B = molar liquid holdup of reboiler, mol
H_D = molar liquid holdup of condenser, mol
h_B = normalized liquid holdup of reboiler, $h_B \equiv H_B/NH$
h_D = normalized liquid holdup of condenser, $h_D \equiv H_D/NH$
j = index of response mode of linearized model with $j=1$ for the slowest mode
k = index of equilibrium stage counted from bottom with reboiler numbered as stage 0

k_s = stagnation point (in terms of stage number) at which $u=0$
L = molar flow rate of liquid stream in rectifying section or any section in general, mol/s; for ion exchange, liquid flow rate, m^3/s
$\overline{L}$ = molar flow rate of liquid stream in stripping section, mol/s
M = number of plates in stripping section, feed plate location
N = number of plates in entire column
q = feed status parameter (liquid fraction or extent of subcooling or superheating) defined by McCabe and Thiele (1925)
R = reflux ratio, $R \equiv L/D$
r = molar holdup ratio of vapor to liquid on each plate, $r \equiv G/H$; for ion exchange, ratio of counterion holdup of exchanger phase to that of liquid phase
S = reboil ratio, $S \equiv \overline{V}/B$
t = time, s
u = normalized wave velocity for specific composition, $u \equiv (\partial\sigma/\partial\tau)_{x \text{ or } y}$
u_Δ = normalized shock wave velocity of self-sharpening wave, $u_\Delta \equiv (\partial\sigma/\partial\tau)_\Delta$
V = molar flow rate of vapor stream in rectifying section or any section in general, mol/s; for ion exchange, flow rate of exchanger stream in moving bed, m^3/s
$\overline{V}$ = molar flow rate of vapor stream in stripping section, mol/s
v^o = linear velocity of bulk liquid flow in fixed-bed ion exchange, m/s
v_x = wave velocity for specific concentration value x, m/s
v_Δ = shock wave velocity of self-sharpening wave, m/s
W = perturbation of w from initial steady-state value w^o
w = normalized holdup of light component in the entire distillation unit, defined by Eq. 9
X = perturbation of x from initial steady-state value x^o
x = liquid mole fraction of light component; for ion exchange, liquid-phase mole fraction of counterion of higher affinity to exchanger
x^o = initial steady-state value of x
x_s = representative liquid mole fraction corresponding to stagnation point of self-sharpening standing wave; x_{sS} for stripping section and x_{sR} for rectifying section
y = vapor mole fraction of light component; for ion exchange, exchanger-phase mole fraction of counterion of higher affinity to exchanger
y^o = initial steady-state value of y
y^∞ = final steady-state value of y
y_s = representative vapor mole fraction corresponding to stagnation point of self-sharpening standing wave
Z_F = feed composition disturbance measured from initial steady-state value z_F^o
z = distance from liquid feed entrance of ion-exchange fixed bed, m
z_F = overall mole fraction of light component in feed (possibly in two phases)
z_F^o = initial steady-state value of z_F

Greek letters

α = relative volatility of light to heavy component; for ion exchange, separation factor of counterion of higher affinity to that of lower affinity
Δ = prefix for difference between two sides of self-sharpening wave
δ = prefix for difference between final and initial steady-state values, or for magnitude and direction (by sign) of disturbance
θ_j = time constant (in normalized time unit) of response mode j of linearized model
σ = normalized distance from bottom of column, $\sigma \equiv k/N$
τ = normalized time, $\tau \equiv tF/NH$

Literature Cited

Alsop, A. W., and T. F. Edgar, "Nonlinear Control of a High-Purity Distillation Column by the Use of Partially Linearized Control Variables," *Comput. Chem. Eng.*, **14**, 665 (1990).

Bowman, J. R., and R. C. Briant, "Theory of the Performance of Packed Rectifying Columns," *Ind. Eng. Chem.*, **39**, 745 (1947).

Boyd, D. M., "Fractionation Column Control," *Chem. Eng. Prog.*, **71**, 55 (1975)

DeLorenzo, F., G. Guardabassi, A. Locatelli, and S. Rinaldi, "On the Asymmetric Behavior of Distillation Systems," *Chem. Eng. Sci.*, **27**, 1211 (1972).

Douglas, J. M., A. Jafarey, and R. Seemann, "Short-Cut Techniques for Distillation Column Design and Control: 2. Column Operability and Control," *Ind. Eng. Chem. Proc. Des. Dev.*, **18**, 203 (1979).

Fuentes, C., and W. L. Luyben, "Control of High-Purity Distillation Columns," *Ind. Eng. Chem. Proc. Des. Dev.*, **22**, 361 (1983).

Gilles, E. D., and B. Retzbach, "Reduced Models and Control of Distillation Columns with Sharp Temperature Profiles," *Proc. IEEE Conf. Decision & Control*, Vol. 2, p. 860 (1980).

Gilles, E. D., and B. Retzbach, "Reduced Models and Control of Distillation Columns with Sharp Temperature Profiles," *IEEE Trans. Auto. Control*, **28**, 628 (1983).

Glueckauf, E., "Principles of Operation of Ion-Exchange Columns," *Ion Exchange and Its Applications*, Soc. Chem. Ind., London, England, p. 34 (1955).

Gould, L. A., *Chemical Process Control: Theory and Applications*, Addison-Wesley, Reading, MA, Chaps. 1, 6 (1969).

Helfferich. F., "Theories of Ion-Exchange Column Performance: A Critical Study," *Angew. Chem. Int. Edit.*, **1**, 440 (1962).

Helfferich, F., "Chromatographic Behavior of Interfering Solutes: Conceptual Basis and Outline of a General Theory," *Adv. Chem. Ser.*, No. 79, 30 (1968).

Helfferich. F., and G. Klein, *Multicomponent Chromatography: Theory of Interference*, Marcel Dekker, New York (1970).

Hwang, Y.-L., "Dynamics of Continuous Countercurrent Mass-Transfer Processes: I. Single-Component Linear Systems," *Chem. Eng. Sci.*, **42**, 105 (1987).

Hwang, Y.-L., and F. G. Helfferich, "Dynamics of Continuous Countercurrent Mass-Transfer Processes: II. Single-Component Systems with Nonlinear Equilibria," *Chem. Eng. Sci.*, **43**, 1099 (1988).

Hwang, Y.-L., and F. G. Helfferich, "Nonlinear Waves and Asymmetric Dynamics of Countercurrent Separation Processes," *AIChE J.*, **35**, 690 (1989).

Jaswon, M. A., and W. Smith, "Countercurrent Transfer Processes in the Nonsteady State," *Proc. Roy. Soc. London*, **A225**, 226 (1954).

Kapoor, N., and T. J. McAvoy, "An Analytical Approach to Approximate Dynamic Modeling of Distillation Towers," *Ind. Eng. Chem. Res.*, **26**, 2473 (1987).

Kapoor, N., T. J. McAvoy, and T. E. Marlin, "Effect of Recycle Structure on Distillation Tower Time Constants," *AIChE J.*, **32**, 411 (1986).

Kim, C., and J. C. Friedly, "Approximate Dynamic Modeling of Large Staged Systems," *Ind. Eng. Chem. Proc. Des. Dev.*, **13**, 177 (1974).

Lamb, D. E., R. L. Pigford, and D. W. T. Rippin, "Dynamic Characteristics and Analogue Simulation of Distillation Columns," *AIChE Symp. Ser.*, **57**, No. 36, 132 (1961).

Luyben, W. L.,"Control of Distillation Columns with Sharp Temperature Profiles," *AIChE J.*, **17**, 713 (1971).

Luyben, W. L., "Profile Position Control of Distillation Columns with Sharp Temperature Profiles," *AIChE J.*, **18**, 238 (1972).

Marquardt, W., "Model Reduction Techniques for Separation Columns," *Proc. Int. Conf. Industrial Process Modeling and Control*, Hangzhou, China (June 6-9, 1985).

Marquardt, W., "Nonlinear Model Reduction for Binary Distillation," *IFAC Proc. Dynamics and Control of Chemical Reactors and Distillation Columns*, 123 (1988).

McCabe. W. L., and E. W. Thiele, "Graphical Design of Fractionating Columns," *Ind. Eng. Chem.*, **17**, 605 (1925).

Mizuno, H., Y. Watanabe, Y. Nishimura, and M. Matsubara, "Asymmetric Properties of Continuous Distillation Column Dynamics," *Chem. Eng. Sci.*, **27**, 129 (1972).

Moczek, J. S., R. E. Otto, and T. J. Williams, "Approximation Models for the Dynamic Response of Large Distillation Columns," *Chem. Eng. Prog. Symp. Ser.*, **61**, No. 55, 136 (1965).

Mohr, C. M. "Effect of the Equilibrium Relationship on the Dynamic Characteristics of Distillation Column Sections," *AIChE J.*, **11**, 253 (1965).

Nandakumar, K., and R. P. Andres, "Minimum Reflux Conditions: I. Theory; II. Numerical Solution," *AIChE J.*, **27**, 450 and 460 (1981).

Rhee, H.-K., R. Aris, and N. R. Amundson, "On the Theory of

Multicomponent Chromatography," *Phil. Trans. Roy. Soc.*, **A267**, 419 (1970).
Rose, A., C. L. Johnson, T. J. Williams, "Transients and Equilibration Time in Continuous Distillation," *Ind. Eng. Chem.*, **48**, 1173 (1956).
Rutishauser, H., "Solution of Eigenvalue Problems with LR Transformation," *Nat. Bur. Standards Appl. Math. Ser.*, **49**, 47 (1958).
Silberberger, F., "Simulation and Control of an Extractive Distillation Column," *Proc. Symp. Comput. Chem. Eng.*, 415 (1977).
Skogestad, S., and M. Morari, "The Dominant Time Constant for Distillation Columns," *Comput. Chem. Eng.*, **11**, 607 (1987).
Skogestad, S. and M. Morari, "LV Control of a High-Purity Distillation Column," *Chem. Eng. Sci.*, **43**, 33 (1988).
Stathaki, A., D. A. Mellichamp, and D. E. Seborg, "Dynamic Simulation of a Multicomponent Distillation Column with Asymmetric Dynamics," *Can. J. Chem. Eng.*, **63**, 510 (1985).
Vermeulen, T., "Separation by Adsorption Methods," *Adv. Chem. Eng.*, **2**, 147 (1958).
Vermeulen, T., G. Klein, N. K. Hiester, "Adsorption and Ion Exchange," *Perry's Chemical Engineers' Handbook*, 6th ed., R. H. Perry, D. W. Green, and J. O. Maloney, eds., McGraw-Hill, New York, Sec. 16 (1984).
Weigand, W. A., A. K. Jhawar, and T. J. Williams, "Calculation Method for the Response Time to Step Inputs for Approximate Dynamic Models of Distillation Columns," *AIChE J.*, **18**, 1243 (1972).

Appendix: Linearized Model

Linearized stagewise model

For demonstrating the limitation of linearized models, the stagewise model listed in Table 1 is linearized in a conventional way for the responses to feed composition disturbances. With reference to an initial steady-state profile $\{x_k^o\}$, the linearized model is written in terms of the following perturbation variables, as functions of the normalized time τ:

$$X_k(\tau) \equiv x_k(\tau) - x_k^o \qquad Z_F(\tau) \equiv z_F(\tau) - z_F^o \tag{A1}$$

The nonlinear equilibrium relation $y_k = f(x_k)$ is linearized as follows:

$$f(x_k) - f(x_k^o) \approx f'(x_k^o)(x_k - x_k^o) \tag{A2}$$

In addition, $f'(x_k)$ resulting from converting dy_k/dt to dx_k/dt is approximated by $f'(x_k^o)$. This conventional linearization approach results in the following matrix equation with a tridiagonal coefficient matrix:

$$\begin{bmatrix} dX_0/d\tau \\ dX_1/d\tau \\ \cdot \\ \cdot \\ dX_M/d\tau \\ \cdot \\ \cdot \\ dX_N/d\tau \\ dX_{N+1}/d\tau \end{bmatrix} + \begin{bmatrix} d_0 & e_0 & & & & & & & \\ c_1 & d_1 & e_1 & & & & & & \\ & \cdot & \cdot & \cdot & & & & 0 & \\ & & \cdot & \cdot & \cdot & & & & \\ & & & c_M & d_M & e_M & & & \\ & & & & \cdot & \cdot & \cdot & & \\ & & 0 & & & \cdot & \cdot & \cdot & \\ & & & & & & c_N & d_N & e_N \\ & & & & & & & c_{N+1} & d_{N+1} \end{bmatrix} \times \begin{bmatrix} X_0 \\ X_1 \\ \cdot \\ \cdot \\ X_M \\ \cdot \\ \cdot \\ X_N \\ X_{N+1} \end{bmatrix} = \begin{bmatrix} 0 \\ 0 \\ \cdot \\ \cdot \\ b_M Z_F(\tau) \\ \cdot \\ \cdot \\ 0 \\ 0 \end{bmatrix} \tag{A3}$$

where the index $N+1$ denotes the total condenser (with subscript D in Table 1). The elements of the tridiagonal matrix are related to the initial steady-state profile $\{x_k^o\}$ as follows:

$$\begin{aligned}
&k=0: && d_0 \equiv \left(\frac{N}{F}\right)\frac{B+\overline{V}f'(x_0^o)}{h_B} && e_0 \equiv -\left(\frac{N}{F}\right)\frac{B}{h_B} \\
&k<M: && c_k \equiv -\left(\frac{N}{F}\right)\frac{\overline{V}f'(x_{k-1}^o)}{1+rf'(x_k^o)} && d_k \equiv \left(\frac{N}{F}\right)\frac{\overline{L}+\overline{V}f'(x_k^o)}{1+rf'(x_k^o)} && e_k \equiv -\left(\frac{N}{F}\right)\frac{\overline{L}}{1+rf'(x_k^o)} \\
&k=M: && c_M \equiv -\left(\frac{N}{F}\right)\frac{\overline{V}f'(x_{M-1}^o)}{1+rf'(x_M^o)} && d_M \equiv \left(\frac{N}{F}\right)\frac{\overline{L}+Vf'(x_M^o)}{1+rf'(x_M^o)} && e_M \equiv -\left(\frac{N}{F}\right)\frac{L}{1+rf'(x_M^o)} \\
&k>M: && c_k \equiv -\left(\frac{N}{F}\right)\frac{Vf'(x_{k-1}^o)}{1+rf'(x_k^o)} && d_k \equiv \left(\frac{N}{F}\right)\frac{L+Vf'(x_k^o)}{1+rf'(x_k^o)} && e_k \equiv -\left(\frac{N}{F}\right)\frac{L}{1+rf'(x_k^o)} \\
&k=N+1: && c_{N+1} \equiv -\left(\frac{N}{F}\right)\frac{Vf'(x_N^o)}{h_D} && d_{N+1} \equiv \left(\frac{N}{F}\right)\frac{V}{h_D}
\end{aligned} \tag{A4}$$

Also, the coefficient for the feed composition disturbance is defined as:

$$b_M \equiv \frac{N}{1+rf'(x_M^o)} \tag{A5}$$

If the condenser holdup is negligible compared with the total column holdup, the $(N+1)$th row of Eq. A3 and the $(N+1)$th column of the coefficient matrix can be dropped with d_N being modified as follows:

$$d_N \equiv \left(\frac{N}{F}\right)\frac{L+Df'(x_N^o)}{1+rf'(x_N^o)} \tag{A6}$$

Equations A3 to A6 are written in a form for a fractionating column shown by Figure 1a, but they can be applied to a rectifying column as shown by Figure 1c or a stripping column with only slight adjustments of the coefficients at the column ends.

Steady-state gains

The steady-state gains of this linearized model with respect to feed composition changes can be obtained by considering a step change $Z_F(\tau)=\delta z_F$. With such a step disturbance, the steady-state gain in terms of liquid composition, $\delta x_k/\delta z_F$, is the ratio of the final perturbation to the step change: $X_k(\infty)/\delta z_F$. Applying Laplace transformation to the matrix equation (Eq. A3) and then utilizing the final-value theorem (for $\tau\to\infty$) leads to the following matrix equation for the gains:

$$\begin{bmatrix} d_0 & e_0 & & & & & & \\ c_1 & d_1 & e_1 & & & & & \\ & \cdot & \cdot & \cdot & & 0 & & \\ & & \cdot & \cdot & \cdot & & & \\ & & & c_M & d_M & e_M & & \\ & & & & \cdot & \cdot & \cdot & \\ & 0 & & & \cdot & \cdot & \cdot & \\ & & & & & c_N & d_N & e_N \\ & & & & & & c_{N+1} & d_{N+1} \end{bmatrix} \begin{bmatrix} \delta x_0/\delta z_F \\ \delta x_1/\delta z_F \\ \cdot \\ \cdot \\ \delta x_M/\delta z_F \\ \cdot \\ \cdot \\ \delta x_N/\delta z_F \\ \delta x_{N+1}/\delta z_F \end{bmatrix} = \begin{bmatrix} 0 \\ 0 \\ \cdot \\ \cdot \\ b_M \\ \cdot \\ \cdot \\ 0 \\ 0 \end{bmatrix} \tag{A7}$$

This set of linear equations can be solved easily by a tridiagonal algorithm. For a rectifying column, the steady-state gains in terms of vapor composition, $\delta y_k/\delta z_F$, may be more convenient. According to Eq. A2, such gains can be related to $\delta x_k/\delta z_F$ by:

$$\delta y_k/\delta z_F = f'(x_k^o)\,(\delta x_k/\delta z_F) \tag{A8}$$

Time constants

The linearized stagewise model described by the $N+2$ equations (less equations for degenerate cases) in Eq. A3 has $N+2$ time constants θ_j, which are the reciprocals of the eigenvalues of the tridiagonal coefficient matrix (Mohr, 1965). These eigenvalues can be efficiently obtained by applying the LR transformation (Rutishauser, 1958) to the tridiagonal matrix iteratively until the subdiagonal elements virtually vanish; then, the diagonal elements of the final bidiagonal matrix are the eigenvalues. The response of each stage consists of $N+2$ response modes, each associated with a time constant. Normally, the largest two time constants dictates the dynamic behavior of such a stagewise process, as discussed by Kim and Friedly (1974). For a high-purity column, the largest time constant θ_1 is usually much larger than the others, as exemplified by the 40-plate rectifying column and the 50-plate fractionating column listed in Table 3. Thus, the transient behavior of a high-purity column is dictated by θ_1 alone, which may be viewed as the time constant of a first-order-lag-plus-dead-time approximation; the dead time is usually much smaller than θ_1 since it is approximately equal to the sum of the other time constants with an adjustment for the distance between the stage of interest and the feed plate (Kim and Friedly, 1974).

Pulse responses

The normalized holdup of the light component in the entire distillation unit, w, defined by Eq. 9 provides a convenient measure for monitoring the response to pulse disturbances. For the linearized model, the perturbation of w from its initial steady-state value w^o can be related to $\{X_k\}$ as follows:

$$W \equiv w - w^o = h_B X_0 + \frac{1}{N}\sum_{k=1}^{N}[1+rf'(x_k^o)]X_k + h_D X_{N+1} \tag{A9}$$

This equation implies that the dynamics of W is characterized by the same set of time constants as for each X_k. Thus, for the response of a high-purity column to a small pulse (ideally, an impulse) disturbance, the decay of the response pulses may be approximated by an exponential decay (first-order lag) with a time constant θ_1.

Manuscript received Nov. 6, 1990, and revision received Mar. 12, 1991.